OCEANS AND ATMOSPHERE
www.csiro.au

Characterisation of Regional Fluxes of Methane in the Surat Basin, Queensland

Interim report on Task 3: Broad scale application of methane detection, and Task 4: Methane emissions enhanced modelling.

Milestone 3.2: ·Model development and analysis of continuous data. Periodic monitoring and field validation.

Milestone 4.1: New data prepared. Milestone 4.2: Data screened, assessed.

D. Etheridge, A. Luhar, Z. Loh, J. Noonan, D. A. Spencer, S. Day, M. Hibberd, S. Zegelin, M. Kitchen, D. Thornton, R. Gregory, P. Krummel, B. Halliburton and D. Barrett

March 2017

Report Title: Characterisation of Regional Fluxes of Methane in the Surat Basin, Queensland

ISBN (print): 978-1-4863-0904-7

ISBN (online): 978-1-4863-0905-4

The Gas Industry Social and Environmental Research Alliance (GISERA) undertakes publicly-reported research that addresses the socio-economic and environmental impacts of Australia's natural gas industries.

GISERA was co-founded by CSIRO and Australia Pacific LNG in July 2011. For further information visit gisera.csiro.au.

Citation

D. Etheridge, A. Luhar, Z. Loh, J. Noonan, D. A. Spencer, S. Day, M. Hibberd, S. Zegelin, M. Kitchen, D. Thornton, R. Gregory, P. Krummel, B. Halliburton and D. Barrett (2017) Characterisation of Regional Fluxes of Methane in the Surat Basin, Queensland. Interim report on Task 3: Broad scale application of methane detection, and Task 4: Methane emissions enhanced modelling report to the Gas Industry Social and Environmental Research Alliance (GISERA). March 2017. CSIRO, Canberra.

Copyright

Important disclaimer

Contents

Acknowledgments ii
Executive summary iii
1 Introduction 6
2 Continuous ground-based methane monitoring 7
3 Filtering for nearby cattle 12
3.1 Confirmation of the effectiveness of the cattle-signal filter 12
3.2 Filtered and selected data set for model interpretation 17
4 Data analysis 19
4.1 Burncluith and Ironbark data analysis 19
5 Atmospheric dispersion modelling for source estimation 27
5.1 Modelling approaches 27
5.2 Backward dispersion modelling at regional scale 28
5.3 Model setup for source inversion 30
5.4 Comparison of modelled winds with data 31
5.5 Modelled backward plume footprints 36
5.6 Background concentration 36
5.7 Emission determination 37
6 Mobile ground surveys 43
7 Preparation of methane emissions inventory 44
8 Discussion, conclusions and further work 46
References 48

Acknowledgments

This report was supported by the Gas Industry Social and Environmental Research Alliance (GISERA). GISERA is a collaboration between CSIRO, Commonwealth and state governments and industry established to undertake publicly-reported independent research. The purpose of GISERA is to provide quality assured scientific research and information to communities living in gas development regions focusing on social and environmental topics including: groundwater and surface water, biodiversity, land management, the marine environment, and socio-economic impacts. The governance structure for GISERA is designed to provide for and protect research independence and transparency of research. Visit gisera.org.au for more information about GISERA's governance structure, projects and research findings.

Gordon and Sue McConnachie are thanked for providing access to their land for the Burncluith station and for support in operating the facility.

Executive summary

This interim report describes progress of the GISERA project "Characterisation of Regional Fluxes of Methane in the Surat Basin, Queensland" to March 2017. Specifically:

Task 3, Broad scale application of methane detection. Milestone 3.2: ·Model development and analysis of continuous data. Periodic monitoring and field validation.

Task 4, Methane Emissions Enhanced Modelling, Milestone 4.1: New data prepared, and Milestone 4.2: Data screened, assessed.

The emissions of methane to the atmosphere from the Surat Basin, Queensland, a region of coal seam gas (CSG) activity are the focus of GISERA research in Greenhouse Gas and Air Quality. The aim of this project is to quantify methane emissions across the Surat Basin using a "top-down" analysis, where methane concentration measurements are combined with atmospheric dispersion modelling to infer emissions.

Data are used from two fixed monitoring stations established across a large segment of the Surat Basin, on either side of existing and future-projected CSG activity. Ironbark (to the southwest) and Burncluith (to the northeast) measure near-continuous concentrations of methane and carbon dioxide (and carbon monoxide at Burncluith), as well as meteorological data.

Data are analysed over a year starting when both stations began monitoring in July 2015. Methane data are first filtered to remove transient spikes in concentration caused by occasional cattle passing nearby the monitor inlets, while retaining the underlying variations resulting from sources of likely interest. Further selection of daytime-only measurements for modelling avoids the difficulties of dispersion models representing stable nocturnal meteorological conditions.

Methane concentration roses for each monitoring site show higher concentrations for wind directions emanating from the CSG area. Differences in methane concentration between Ironbark and Burncluith, when the wind is in line with the two stations, provides the background-subtracted concentration differences due mainly to sources between the sites. These differences are typically less than 50 ppb but occasionally 100-200 ppb, compared to a background concentration of about 1800 ppb. These data will be suitable for inferring methane source emissions in the sector between the stations using models.

An inverse modelling technique was developed to infer methane emissions across the broader region using hourly mean concentration measurements at Ironbark and Burncluith, a regional transport model, and a Bayesian inference analysis. The TAPM meteorological model was run in backward mode to obtain hourly source-receptor relationships. Emissions were determined for 18x18 km grid cells across a 200x200 km domain. The inversions gave computationally-stable and consistent solutions from run to run.

Emissions were inferred from the inverse modelling using concentration data from Ironbark, from Burncluith and from both stations jointly in a single Bayesian run. There are similarities in the source distributions inferred by each inversion though it is likely that the joint station result is

more reliable due to the extra information and the spatial separation provided by the two monitoring locations. Even so, there are uncertainties in the inverse modelling that could lead inaccuracies in the inferred source locations and emissions. An indication is that a large, steady and independently measured methane emission does not appear in its expected location in the inverse modelled source distribution, but may appear in adjacent grid cells. Possible causes of uncertainty in the inverse modelling include differences between modelled and observed meteorology across the model domain, assumptions that the source emissions are constant over time, the calculation of background concentration for each site, the attribution of sources to points within a relatively coarse grid, and the small number of monitoring sites compared to many sources across a wide area. Ways to improvements addressing these limitations are considered for future work. Importantly, methane emissions come from a range of source types and the inversions and interpretations of concentration data alone cannot be used to discriminate between them.

An inventory of methane emissions for the region has been compiled with input from a consultant. When completed it will contain all major methane sources gridded to 1 km by 1 km cells across a 345 km by 344 km area centred near Miles, which contains the domain of the inverse modelling. The emissions data are derived from state, national and international databases, from the GISERA and CSIRO mobile methane monitoring activities, and from industry. This “bottom-up” inventory will be used both in forward modelling, to simulate concentrations to compare with measurements at the monitoring stations, and to compare with the “top-down” emissions inferred from the inverse modelling.

1 Introduction

This report describes interim results of the measurements and modelling activities of Phase 3 of the GISERA project "Characterisation of the Regional Fluxes of Methane in the Surat Basin, Queensland".

The project was planned over three main phases. Phase 1 was a survey, review and analysis of the literature on the methods of detection and measurement of methane to quantify methane source locations and fluxes across a region (Day et al., 2013). It recommended that Phase 2 of the project consist of two general components, namely a field survey combining mobile survey and remote sensing methods to establish the location and approximate magnitude of seeps in the Surat Basin, and, to establish an atmospheric measurement station to measure regional background methane fluxes. Phase 2 used atmospheric modelling to identify optimum locations for atmospheric monitoring stations across a CSG-intensive sector of the Surat Basin, from which concentration measurements could be used to infer regional methane emissions using "top-down" techniques (Day et al., 2015). It recommended a minimum of two stations across the CSG area of the Surat Basin and reported on the scoping of sites for stations and the installation and initial results of the first, Ironbark. Phase 3 concentrates on the regional atmospheric monitoring measurements, analysis of data and development and application of model methodologies to infer emissions across the region using an inverse approach. The need for inverse modelling of emissions using multiple stations to detect diffuse sources across a region (order of 100 km) was noted in Phase 1. Note that since the original project order it was agreed to run Phase 3 over three years (originally to be one year), though with similar total funding. This was to allow the baseline monitoring to reveal any seasonal variability or year to year trends in emissions that would be difficult to discern from a 12-month monitoring campaign. The installation, commissioning and operation of the two stations (Ironbark and Burncluith) and preliminary data were described in milestone 3.1 (Etheridge et al., 2016). An additional task, Methane Emissions Enhanced Modelling, was included to handle the additional measurements and modelling development associated with the second station and potentially from the recently installed air quality monitoring stations which included measurements of methane concentration.

The milestones addressed in this interim report therefore include:

- 3.2: Model development and analysis of continuous data. Periodic monitoring and field validation. (Note that the "Trial of remote sensing technologies" task was completed earlier and described in the interim report, milestone 3.1, Etheridge et al., 2016).
- 4.1: Prepare new data from new and emerging monitoring stations, from field surveys including EC fluxes, and of gas tracers.
- 4.2: Evaluate data from 4.1 for ability to determine the local and regional sources of methane. Screen data for non-CSG sources such as livestock and combustion emissions.

2 Continuous ground-based methane monitoring

The monitoring stations were designed to measure near-continuous CH_4 concentrations spanning a large segment of the Surat Basin over several years, to provide a baseline record, to provide upwind-downwind differences, to infer net emissions across that segment, to characterise variations over diurnal and seasonal timescales, and to potentially detect trends. The sites were located to optimise the size and frequency of signals from the broader CSG source area without being overly influenced by potential sources nearby. Atmospheric dispersion models were used to simulate concentration signals based on the local and regional meteorology and scenarios of potential source locations and nominal emissions rates. Practical considerations (such as access and power) were also taken into account. The chosen site locations (Figure 1) were to the southwest (Ironbark) and northeast (Burncluith) of a belt of CSG operations. Mobile monitoring surveys were used to confirm that there were no significant sources in the immediate area before the sites were established. The monitoring strategy is further described in the Phase 2 report (Day et al., 2015).

The Ironbark site is 79 km south-west (217 degrees) of Burncluith, and is located at -27° 8' 6.5" latitude, 150° 14' 37.6" longitude (226.806 km east, 6995.596 km north MGA; Zone 56). Burncluith is located at -26° 34' 2.4" latitude, 150° 42' 5.4" longitude (271.051 km east, 7059.430 km north MGA; Zone 56). The meteorological towers were sited nearby the gas analyser inlet locations with instrument heights above ground of 5.5 m (Ironbark) and 7.5 m (Burncluith).

A baseline atmospheric record would ideally begin before the start of the activity that is required to be monitored. A baseline record also needs to be continuous (minute or higher frequency measurements) and for at least a year to account for diurnal and seasonal variations in the natural and methane fluxes and meteorology (temperature, wind, rainfall) that cause the observed concentrations. Also, many anthropogenic sources are likely to have varying emissions. For example, the numbers and locations of livestock may change during the year and controlled burn-offs can be periodic. Because the atmospheric monitoring described in this report began after many CSG activities were underway, it doesn't provide a true pre-CSG industry baseline. But the concentration and meteorological measurements, beginning in July 2015 for the pair of stations, provide the first continuous independent monitoring from which the total methane emissions can potentially be inferred across the region. Given the increase expected in CSG activities (for example, DNRM 2014), the records provide a relatively early snapshot that could be used to detect changes in net methane emissions across the region in the future.

Figure 1. Google Earth map of the CSG region showing CSIRO/GISERA greenhouse gas monitoring stations (Ironbark and Burncluith), air quality stations and nearby towns and roads.

Monitoring at Ironbark and Burncluith has operated since 8 November 2014 and 15 July 2015 respectively. Gaps in data have usually been caused by power failures and have typically been short (less than a few days at a time). However, more protracted power outages to the Ironbark site have caused extended interruptions from December 2016 to March 2017. The Picarro analyser at Ironbark was replaced after failing in September 2016. The available data when both stations operated now span more than a year (August 2015-July 2016) and will be used in modelling to infer methane sources across the region.

Concentrations of CO_2 and CH_4 are measured at Ironbark and CO_2, CH_4 and CO at Burncluith from 10 metre high inlets. The high frequency data (approx. 0.3 Hz) are quality controlled (flagged out of the record when key instrument parameter stray outside of acceptable operating conditions) and calibrated using CSIRO produced standards. Careful calibration allows the data to be reported on the appropriate World Meteorological Organisation mole fraction scale; NOAA04 for CH_4, WMOX2007 CO_2 scale and the NOAA CO scale. Data are calculated to 1, 5, 20 and 60 minute means. 60 minute means are used in modelling of source emissions with CSIRO's TAPM model. Identical measurement methodology and calibrations allow the concentrations from each site, and from other sites in CSIRO's network (http://ds.data.jma.go.jp/gmd/wdcgg/cgi-bin/wdcgg/accessdata.cgi?lang=&contributor_index=200612120064), to be exactly intercompared in models to infer source emissions. The data reside on the PCs at the sites and on CSIRO servers. The installations are further described in the Milestone 3.1 report (Etheridge et al., 2016).

Concentration records for Ironbark and Burncluith are shown in Figure 2 and Figure 3. Together these data are used to provide background-subtracted concentrations which can be traced to methane emissions from the region between the two analysers, during selected periods when winds are consistent with the strategy described in the Phase 2 report (Day et al., 2015). We further use methane concentrations from the two sites, after background subtraction estimated from the measured CH_4 minima at each station (see below), to infer emissions of methane sources across the region using inverse modelling. Differences in CH_4 concentrations calculated between the sites for steady meteorological conditions will be used to infer the areas and emissions of methane sources in between the sites using another modelling setup.

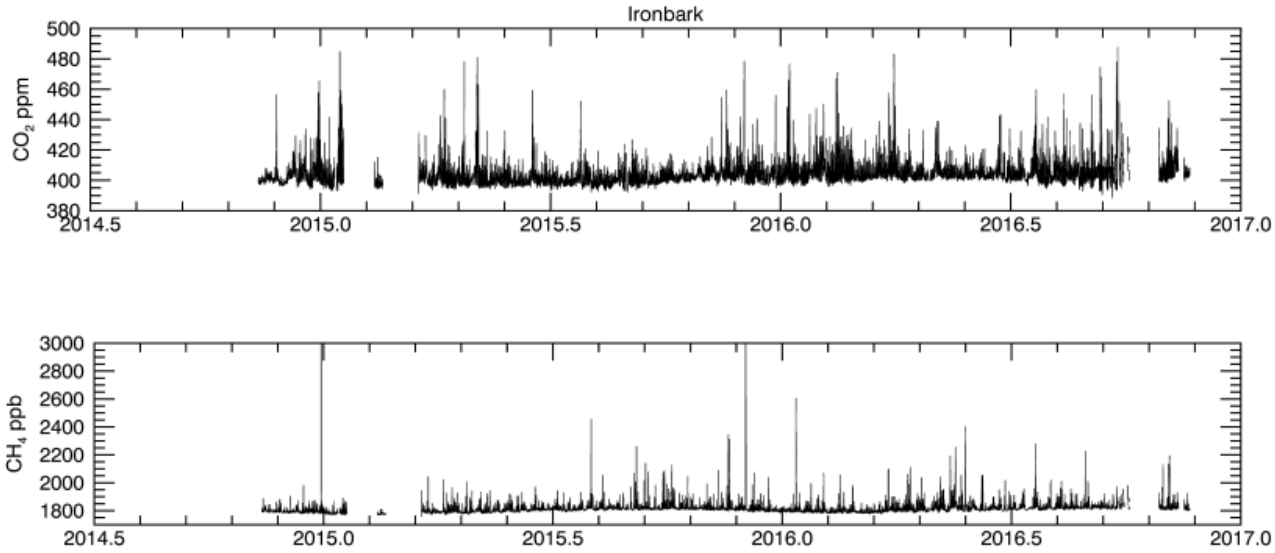

Figure 2 Concentrations (hour means) of CO_2 (parts per million, ppm) and CH_4 (parts per billion, ppb) at Ironbark.

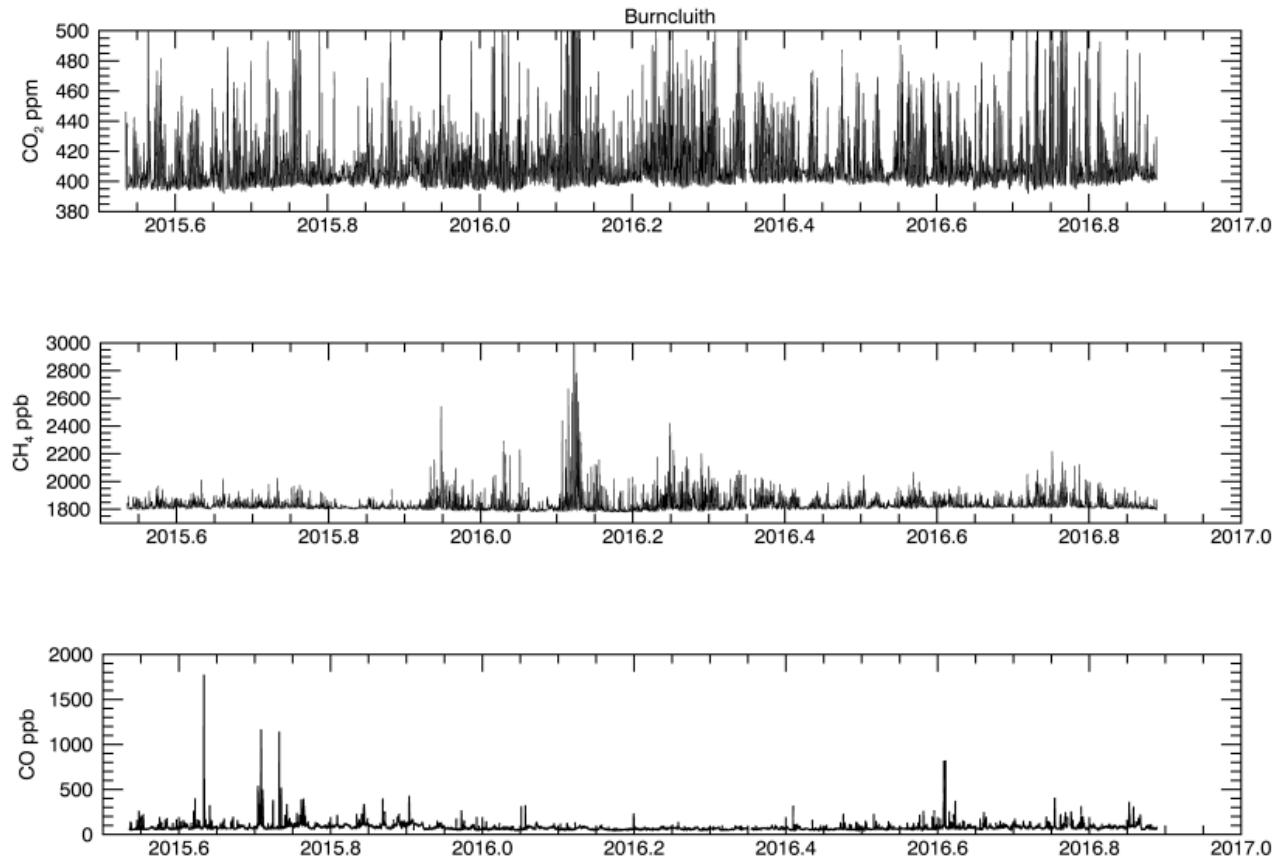

Figure 3 Concentrations (hour means) of CO_2 (ppm), CH_4 (ppb) and CO (ppb) at Burncluith.

Measurements of methane from the GISERA air quality monitoring network can also potentially inform the interpretation and inverse analysis of methane source emissions. The Hopeland station (Figure 1) is approximately midway between Ironbark and Burncluith. However, because it is situated close to sources of potentially large methane emissions, the record is likely to be

dominated by these sources at times. Further, several hundred head of cattle were introduced to this property in late 2015, which have increased methane levels. Inclusion of the methane record from Hopeland for interpretation of the regional scale emissions will depend on suitable filtering of data for the cattle signals (see below) and selection for wind directions that avoid overrepresentation of the nearby sources. The Hopeland methane measurements will also need to be calibrated to the CSIRO scale.

Beginning in the middle of 2016, the facilities at Ironbark and Burncluith have also supported GISERA air quality monitoring (Lawson et al., 2017; https://gisera.org.au/project/ambient-air-quality-in-the-surat-basin/). Measurements include nitrogen oxides (NO_x), ozone (O_3) and carbon monoxide (CO) using instruments operated by Ecotech for CSIRO. Carbon monoxide concentrations at Burncluith are provided by the CSIRO greenhouse gas monitoring instruments.

The air quality and greenhouse gas measurements can be complementary. For example, methane from burning off is likely to have increases in air quality gases such as NO_x and CO, which could be used as tracers to distinguish biomass burning methane from methane from other sources.

3 Filtering for nearby cattle

The strategy used in Phase 2 to identify optimal monitoring station locations suggested that Burncluith is well placed, acting as the up/downwind counterpart to Ironbark, given the dominant seasonal wind regimes and the expected distribution of CSG and other methane sources in the Surat Basin. It also found that there were no significant methane sources in the immediate area that would unduly affect the measurements of regional emissions, other than the dwelling, which is outside of the main wind sectors of interest when Burncluith is used as a counterpart to Ironbark, and cattle. Located on a private farm holding, the land owners run a small number (30-40 head) of cattle in the paddocks adjacent to the monitoring station. Due to the proximity of the cattle, the relative size of their emissions can be potentially significant compared to signals from larger, but more distant sources.

When meteorological conditions are relatively well mixed (typically daytime with moderate or greater wind speeds), the proximity of the local herd ensures that the methane emission signal appears as one or many narrow peaks overlaying the smoother background variability carrying information about more distant sources.

In order to ensure that contributions from proximate cattle would not undermine the value of the Burncluith record as a boundary condition to constrain emissions from the broader Surat Basin – our region of focus – we developed a method to filter the methane record for local cattle emissions, based on their unique temporal characteristics.

Our standard data processing, using the software package GCWerks (http://www.gcwerks.com/), involves manual checks on a number of instrument parameters, but also some automatic flagging procedures based on very conservative thresholds for removing spurious data. In particular, GCWerks removes outlying points in the high frequency data if they lie more than 10 standard deviations from the mean, as calculated over a two minute moving average window. By judiciously modifying the default parameters in the GCWerks' statistical filter, we are able to remove the signal due to the local cattle, without modifying the underlying signal from more distant sources. We find the optimal filter parameters for filtering nearby cattle signal to be a standard deviation of 2.5, with a moving average over a ten minute window. In this way, rapid spikes due to meandering cows (or stationary cows with meandering winds) are removed, without altering the underlying signals and trends in methane concentration.

3.1 Confirmation of the effectiveness of the cattle-signal filter

Through the assistance of the landholders at Burncluith, we have documented many periods of time when there were significant numbers of cattle immediately upwind of the monitoring locations. In addition, the landholders have been very helpful in supplying information regarding use of their wood-fired heater and smoke emissions from nearby controlled burns. Below we show plots of a selection of these periods to demonstrate the effectiveness of our filter at removing close range point source signals (such as cattle and wood heater emissions from the house), while

preserving signals from more distant and significant sources, such as those from biomass burning, and other anthropogenic activities in the Surat Basin more broadly.

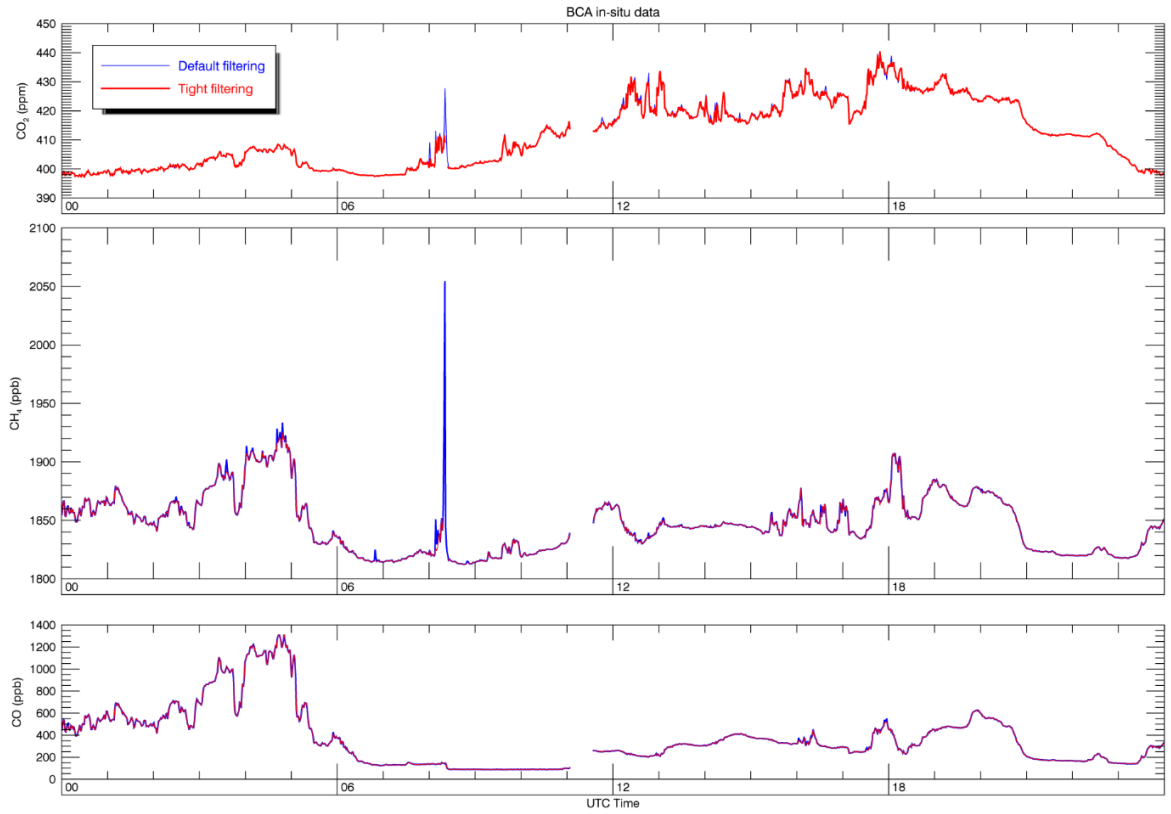

Figure 4. Burncluith minutely-mean data for September 16 2015. Blue curves represent the default filtering, red curves the cow filtering ("tight").

During mid-September 2015, the landholders reported significant smoke emanating from a prescribed burn in the Barakula forest (4 to 40 km north of Burncluith). The combination of elevated CH_4 and CO together is a very strong marker for biomass burning. In the early hours of September 16, 2015 the data show a very strong correlation between the CH_4 and CO. The underlying correlated signal is preserved using the 'tight' or cow signal filtering. Just after 0800 hours, a substantial, but short-lived spike in CH_4 is correlated with the CO_2. The ratio of the signals is approximately 200 ppb (0.2ppm) CH_4 to 15 ppm CO_2, or 0.013. Because cattle emit methane mostly with their breath, we expect cattle methane emissions to be accompanied by a CO_2 signal. Bai et al. (2014) report molar ratios of the order 0.008 – 0.044 CH_4:CO_2 for cattle. The short-lived spikes in our data in Figure 4 are consistent with a local cattle signal, and are successfully removed by the filtering.

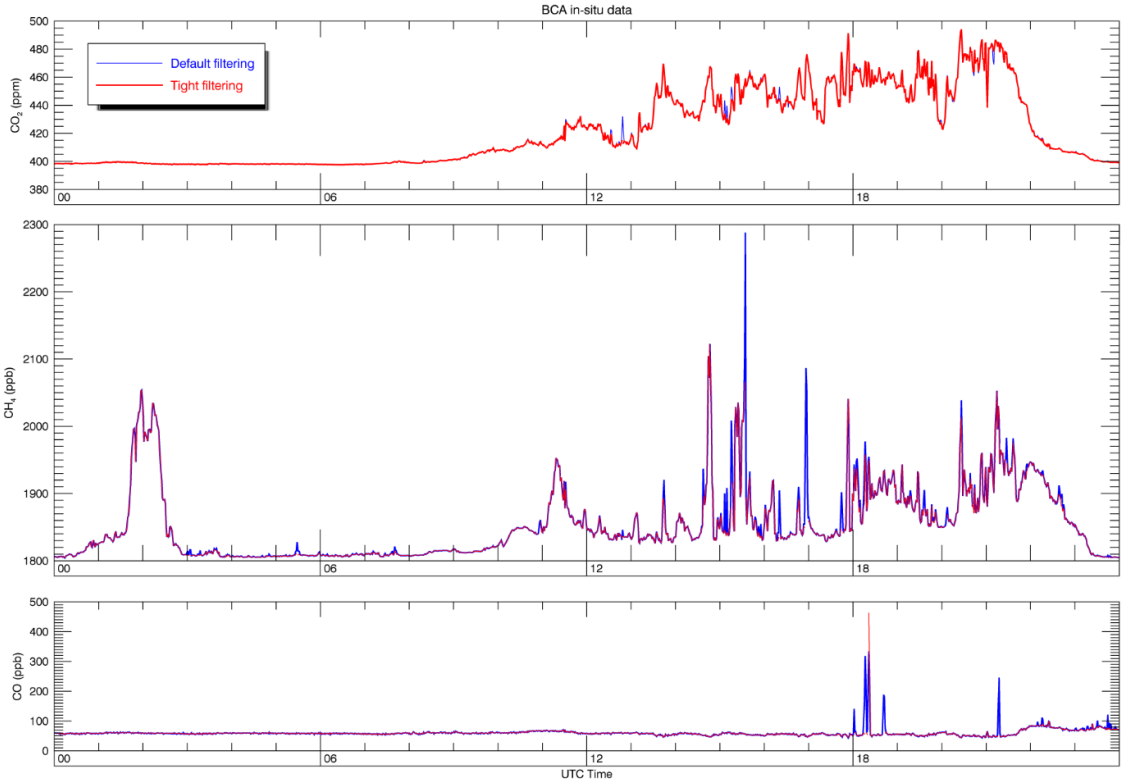

Figure 5. Burncluith minutely-mean data for July 25 2016. Blue curves represent the default filtering, red curves the cow filtering ("tight").

Figure 5 shows Burncluith data for 25 July 2016. While some spikes in CH_4 are filtered out in the period 1500-1800 UTC (0100-0400 AEST), there is a large CH_4 feature from 0230-0330 UTC (mid-morning local time) which is retained in the 'tight' filter. This feature is of particular interest as it is significant in size and duration and has no corresponding CO_2 or CO signal (indicating that it is unlikely to be ruminant or biomass burning emissions). A check with the landholder at this time confirms that there were no cattle in the immediate upwind patch. Therefore, this CH_4 signal is characteristic of the CH_4 signals we wish to retain in our record and seek to understand and our filter handles it correctly. For comparison, later that day, many higher-frequency spikes in CH_4 are removed by the filter. These spikes often had corresponding high CO_2 or CO concentrations, characteristic of emissions from cows or the wood-fired heater.

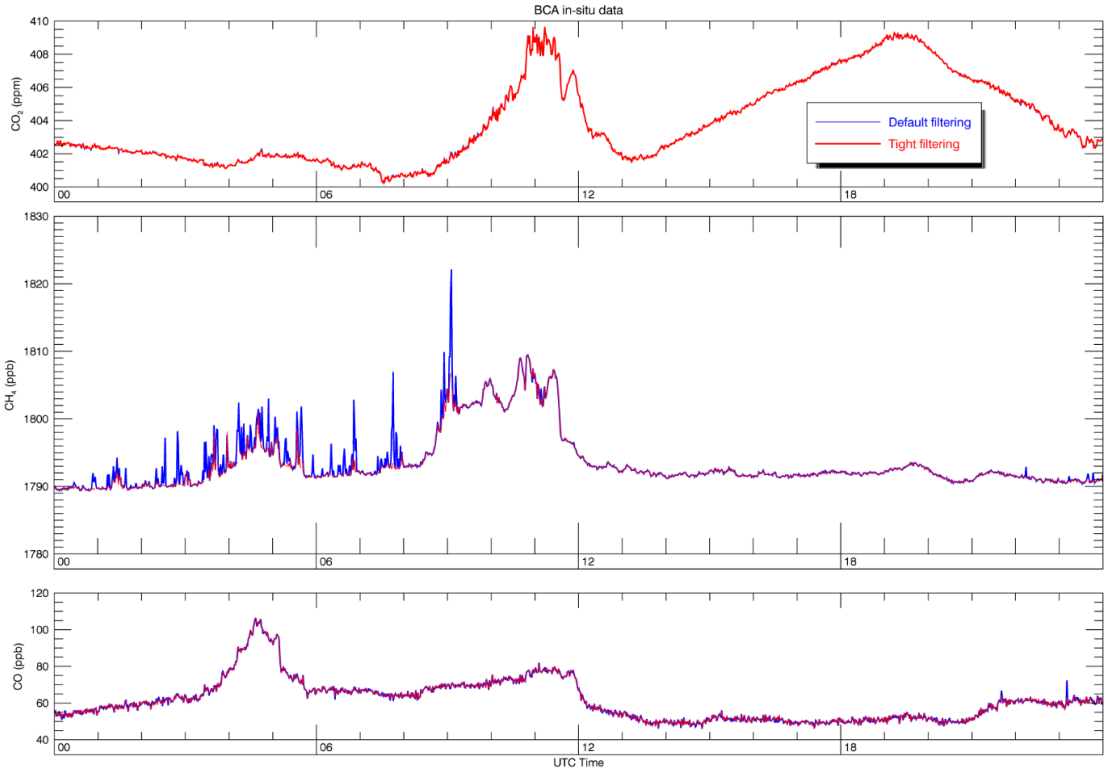

Figure 6. Burncluith minutely-mean data for January 10 2017. Blue curves represent the default filtering, red curves the cow filtering ("tight").

Figure 6 shows the data at Burncluith for 10 January 2017. Particularly from 1200 to 1600 local time (UTC 0200-0600), there is a series of sharp spikes in the CH_4 record. At this time, there were light winds from an east-south-easterly direction, and the landholder confirmed that there were two cows loitering to the east of the intake line. While the 'tight' or cattle filter removes most of these sharp peaks in the minutely data, it retains the underlying rise in CH_4 between 0400 and 0600 UTC which mirrors the rise in CO, suggestive of biomass burning signal being transported from further afield.

The cattle filter behaves as required, removing most large amplitude, high frequency spikes in methane concentrations likely from nearby cows while retaining persistent signals resulting from emissions from sources of possible interest. However, it is not expected to remove signals from the larger population of grazing cattle or feedlots across the region.

The same cattle filter was applied to the Ironbark data, for consistency, although cattle are fewer and further away at Ironbark and have much less impact on the methane measurements. The differences between the default methane data and filtered data for Burncluith and for Ironbark are shown in Figure 7. Note that negative differences (where the cow-signal filter actually produces a bigger hour mean than the default filter) occasionally occur at night time when there is likely to be stable stratification and intermittent mixing, occasionally leading to sharp drops in the methane concentration. Just as the cow-induced spikes get filtered out, meteorologically driven dips also get filtered out. The filter could also be applied to methane concentration data from other sites such as Hopeland.

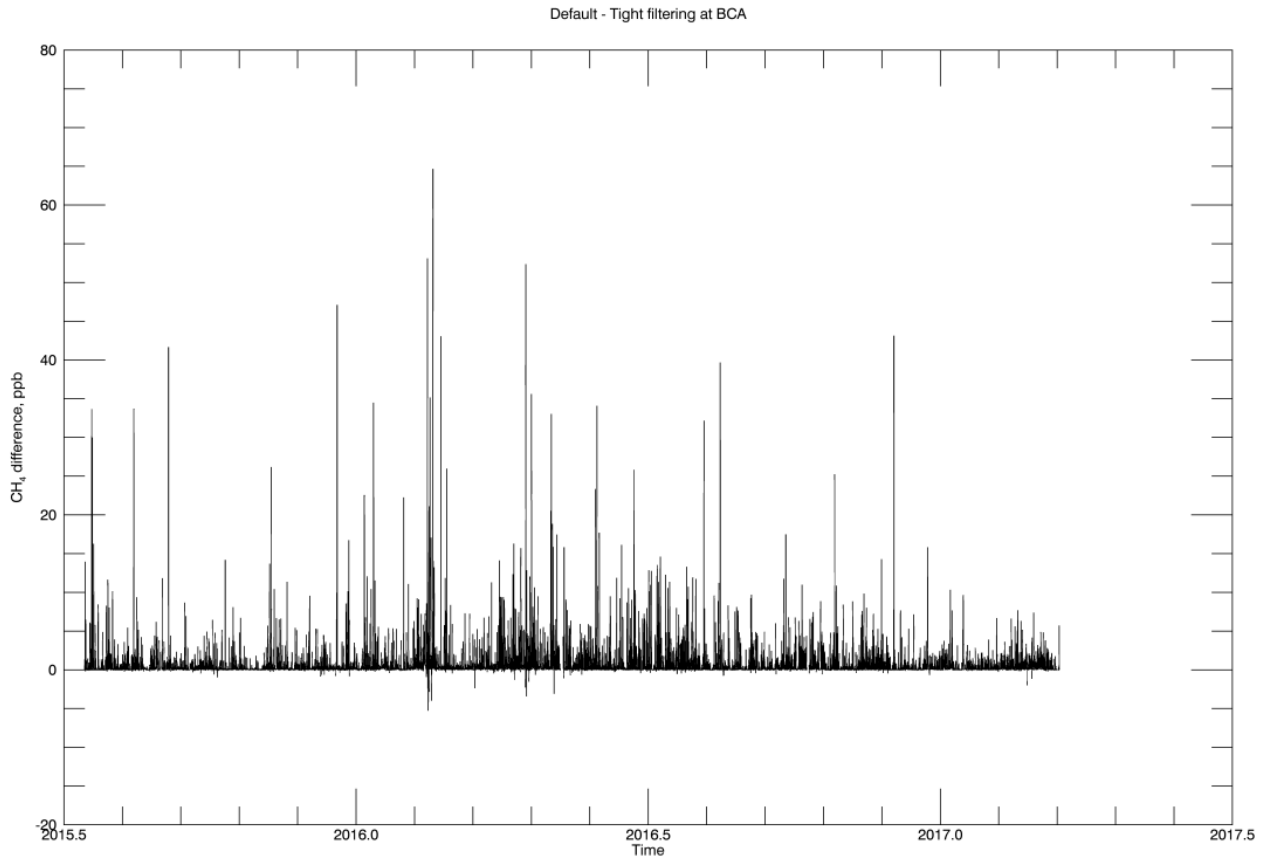
Default - Tight filtering at BCA
80
60
40
20
0
-20
CH4 difference, ppb
2015.5
2016.0
2016.5
2017.0
2017.5
Time

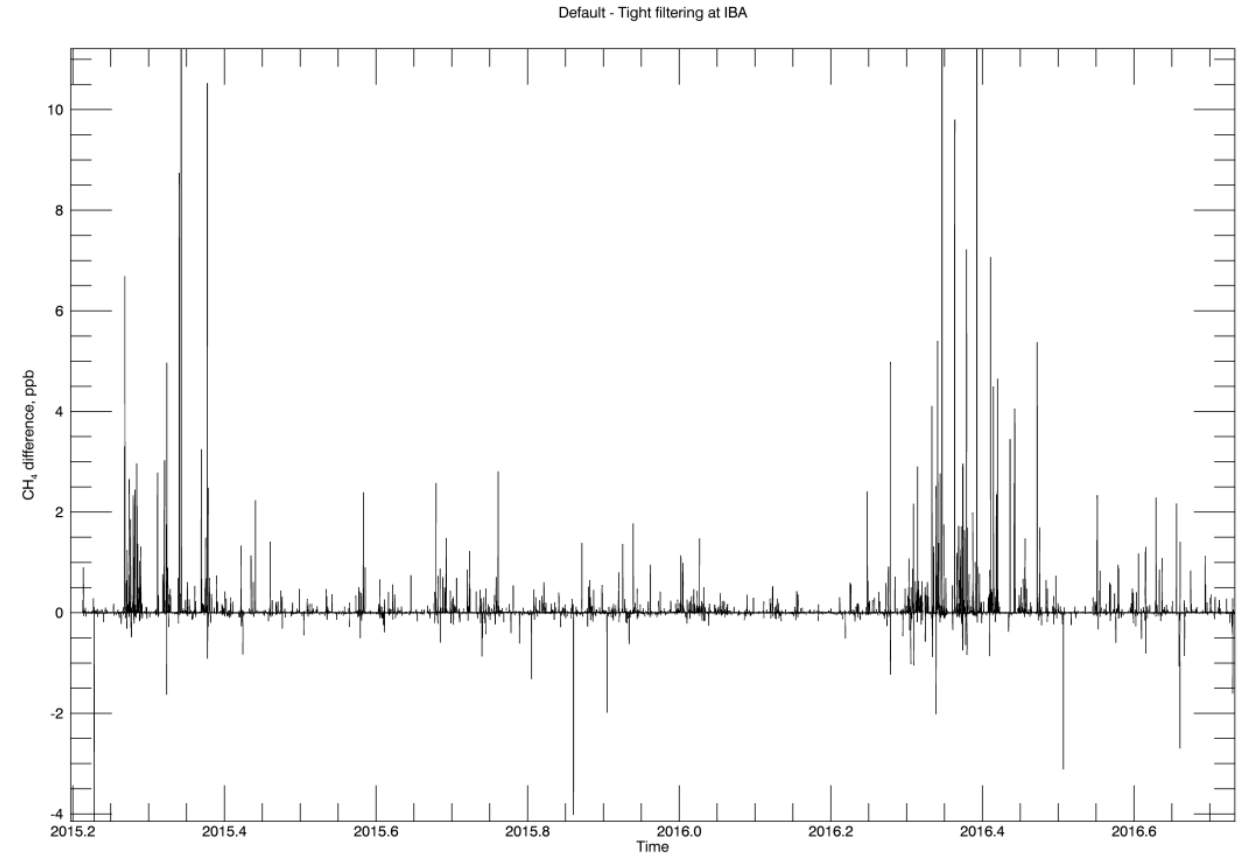
Default - Tight filtering at IBA
10
8
6
4
2
0
-2
-4
CH4 difference, ppb
2015.2
2015.4
2015.6
2015.8
2016.0
2016.2
2016.4
2016.6
Time

Figure 7. Differences between default and cattle-filtered hour-mean methane data for Burncluith (top) and Ironbark (bottom).

3.2 Filtered and selected data set for model interpretation

Based on the above approach, we now use our 'cattle-filtered' data set to find concentration differences between the two sites. Predicted differences between the sites simulated by TAPM were previously used in the design of the monitoring network (Day et al., 2015). Figure 8 shows the difference in hour-mean, filtered methane concentrations between Ironbark and Burncluith for 15 months beginning in July 2015 when both stations began operating.

Concentration differences between the sites were predicted by TAPM model simulations with scenarios of assumed methane emissions for Surat Basin CSG sources only (Figure 6.9 in Day et al., 2015). As expected, the observed methane concentration differences are much larger, mainly because the simulations don't include the many other methane sources in the region and possibly because of differences between the assumed and actual CSG sources. The simulated concentration differences may also be affected by inaccurate representation of dispersion by the model during stable, low wind speed conditions, typically at night time.

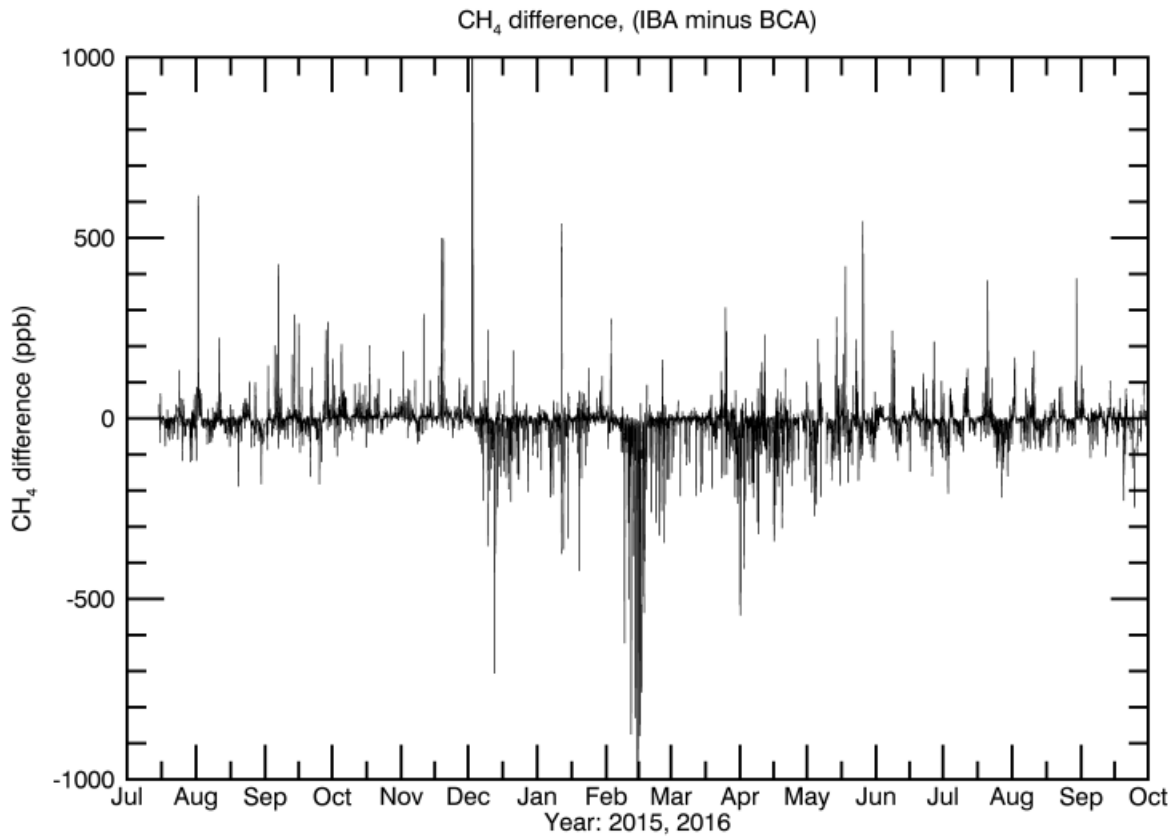

Figure 8. Differences in hour-mean, filtered methane concentrations between Ironbark and Burncluith

In Figure 9, we show the difference dataset between the two sites for the daytime period (0900-1900 AEST). When comparing Figure 8 and Figure 9, it becomes clear that a considerable amount of the differences between the two sites occur during the night time. This is because at night time the atmosphere is typically characterised by stable stratification and a decreased boundary layer

height so that even small local sources can lead to very large enhancements in the local methane concentration because there is little atmospheric mixing. Difficulties in representing dispersion in the models under these conditions can lead to errors (Luhar and Hurley, 2012). Therefore the day-time selected data used in Figure 9 are those which we later use in the data analysis and regional scale modelling.

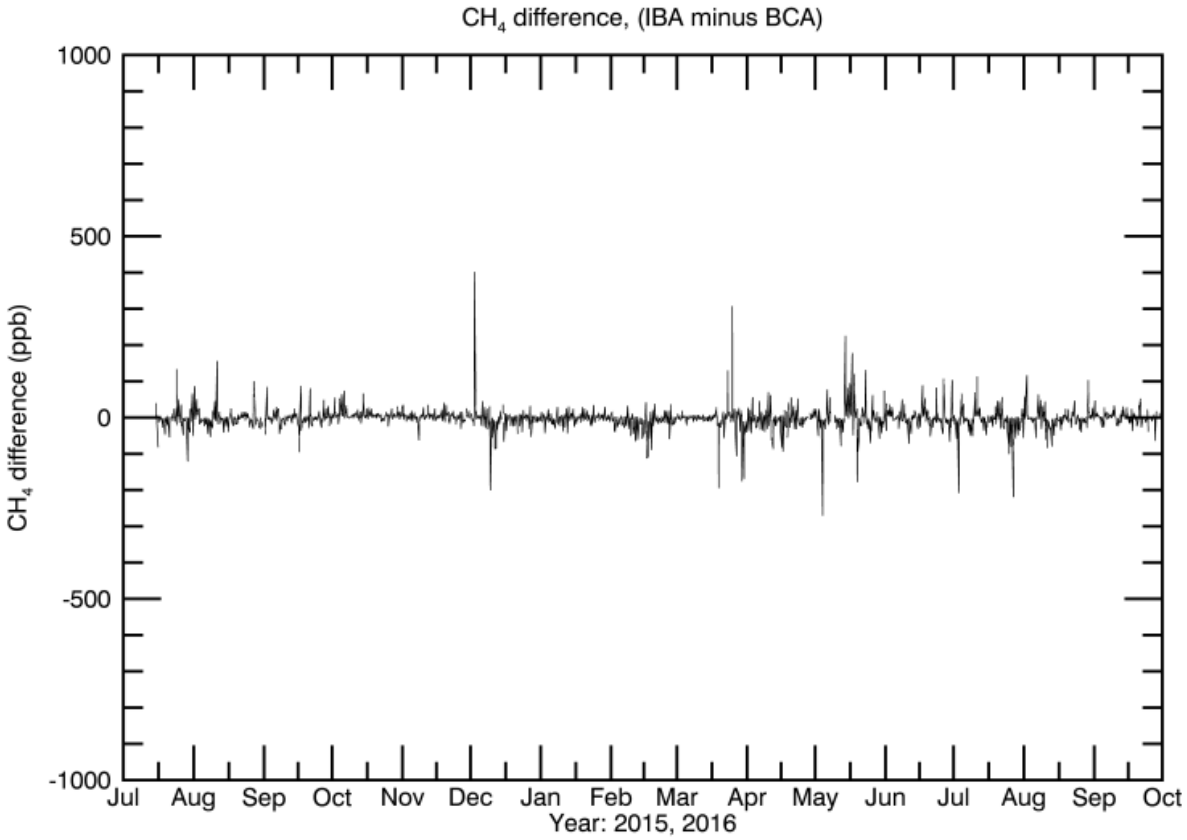

Figure 9. Differences in hour-mean, filtered methane concentrations between Ironbark and Burncluith selected for the period 0900-1900 (end of hour) AEST.

4 Data analysis

In this section we present an analysis of the methane concentration data coupled with measured meteorology. A comparison of the modelled meteorology with the measurements is presented later in the modelling section. The hour mean (with time stamps at the end of the hour in local time), cattle filtered concentration data for each station are used here.

4.1 Burncluith and Ironbark data analysis

Continuous measurements of methane concentration and micrometeorological data started at Ironbark from November 2014 and at Burncluith from July 2015. Simultaneous meteorological and concentration data at both sites for one full year cover the period 16th July 2015 until 15th July 2016 which is therefore the period we have analysed. Figure 10 shows the observed wind roses at Burncluith and Ironbark for 2015 – 2016. The observed wind sectors at Burncluith and Ironbark are generally similar. The wind information at each site was used as input for the siting of the monitoring stations (Day et al., 2015; Etheridge et al., 2016), such that the pair of stations provide upwind-downwind concentrations along the predominant northeast-southwest wind sectors spanning the CSG region.

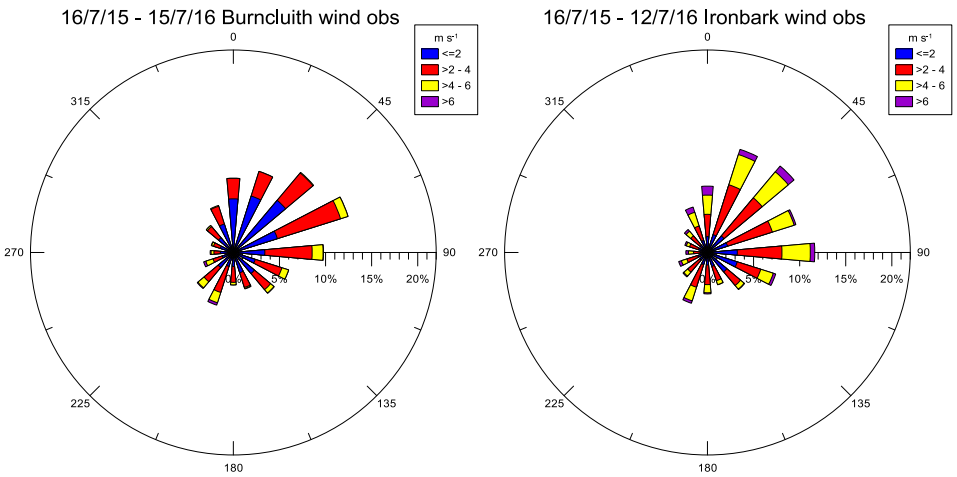

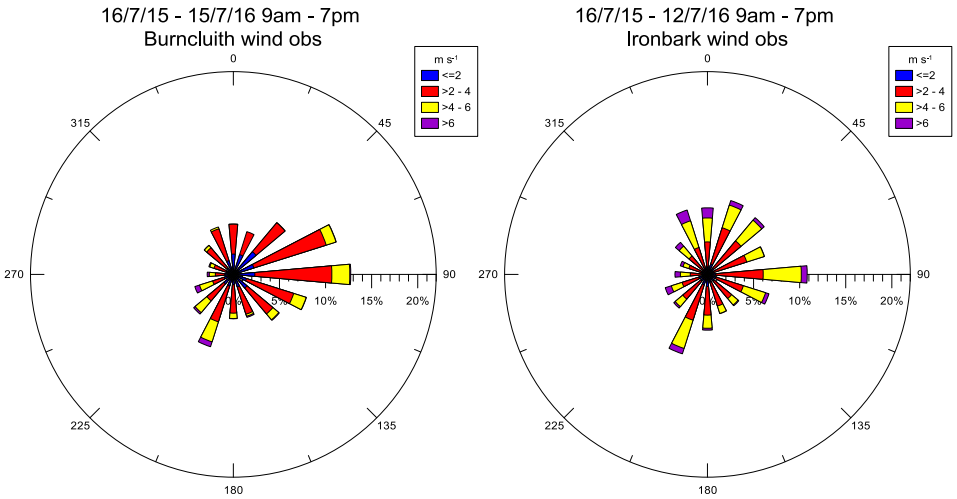

Figure 10. Wind roses for Burncluith and Ironbark for 2015 - 2016 based on observations. The top figures are for all data, the bottom figures are selected for daytime hours.

Figure 11 presents observed monthly-averaged methane concentrations at Burncluith and Ironbark (purple bars) and also the number of hourly observations available for averaging (blue line). The concentrations reflect the seasonal cycle in the background methane but are also affected by local and regional sources. Both sites show an approximate amplitude of 30 ppb for the seasonal cycle. The monthly-averaged CH_4 values at Burncluith are generally larger than those at Ironbark except during September – November. The monthly average of the daily minimum (red line) is also shown at both sites, which is taken as the regional background in the modelling reported later.

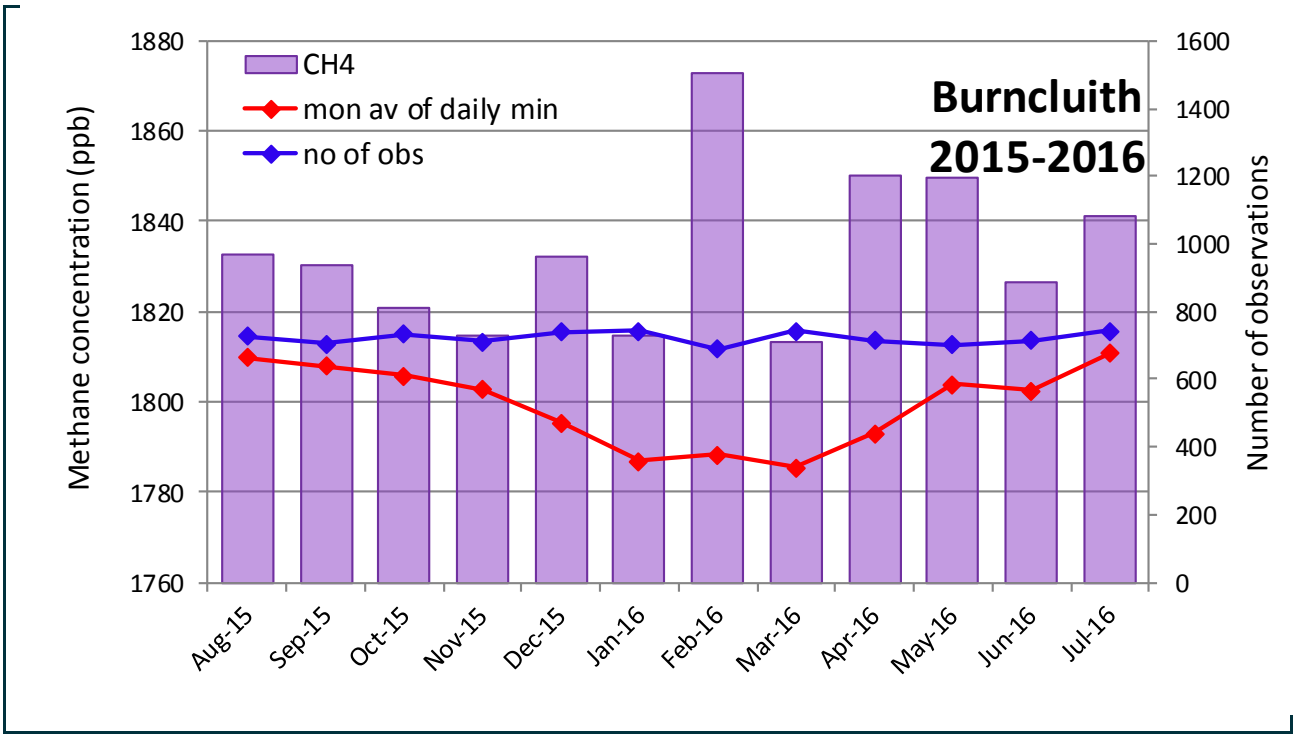

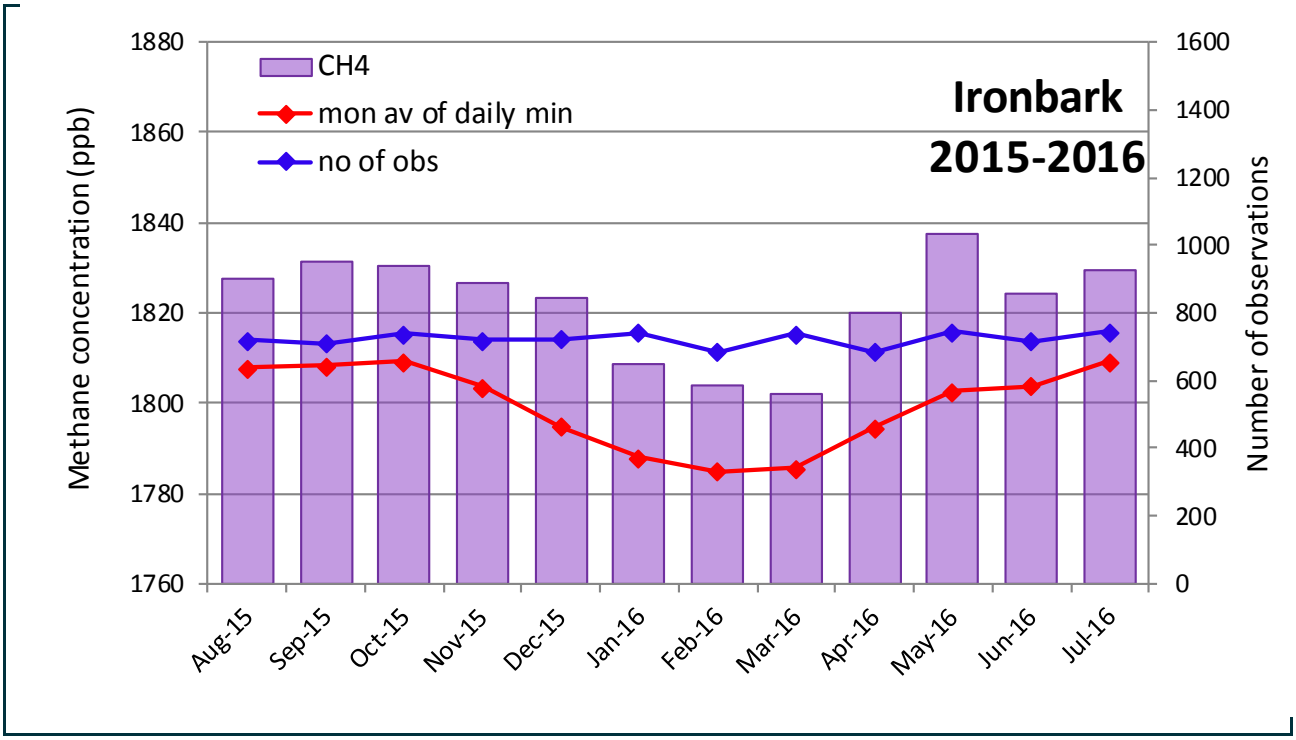

Figure 11. Observed monthly-averaged methane concentration at Burncluith (top) and Ironbark (bottom) for 2015-2016. The number of available hourly observations for each month along with monthly average of the daily minimum is also shown.

Figure 12 shows the methane concentration rose based on the concentration measurements and sonic anemometer wind data at Burncluith and Ironbark. The bottom panels of Figure 12 show the concentration wind roses selected for daytime hours only. High concentration events can occur under all wind directions, but the chances of these events occurring are higher for winds from the north-east sector at both stations and also from the south west at Burncluith.

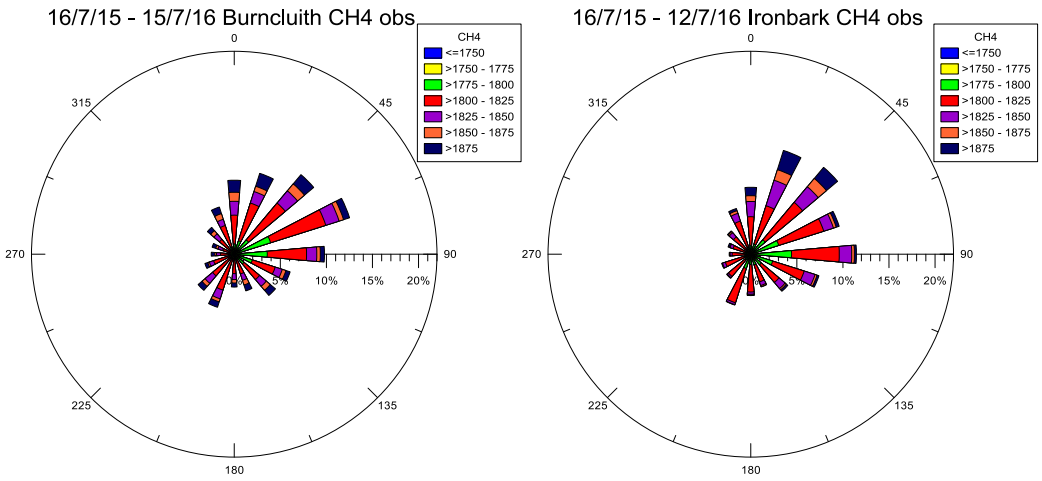

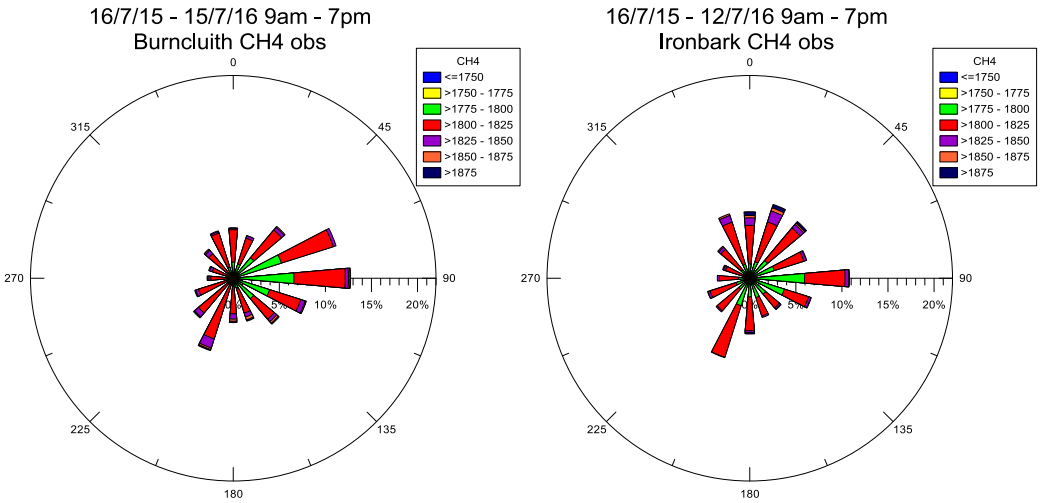

Figure 12. Methane concentration roses for Burncluith and Ironbark for 2015 – 2016 based on the measurements of CH_4 at each station. The top figures are for all data, the bottom figures are selected for daytime hours.

The plots of the observed methane concentration at Burncluith as an averaged function of diurnal hour and wind direction (Figure 13– top plot) and an averaged function of diurnal hour and wind speed (Figure 13 – bottom plot) show high concentration levels during 2000-0800 h for winds from all directions but highest between 90–360 degrees. These events mostly correspond to nocturnal stable conditions with low to moderate wind speeds and shallow atmospheric mixing. Figure 14 shows the same plots for Ironbark. At Ironbark high concentrations occur during 2200-0800 h for winds from predominantly 0–90 and 270–360 degrees. These events also mostly correspond to nocturnal stable conditions with shallow atmospheric mixing, but with higher wind speeds than at Burncluith. Unlike Burncluith the averaged methane concentrations are not as high when the wind has a southerly component. It is also important to note that there are still some hour mean concentration values that are high during the daytime hours but these are masked by the averaging process used in Figure 13 and Figure 14 as they are less frequent than those at night.

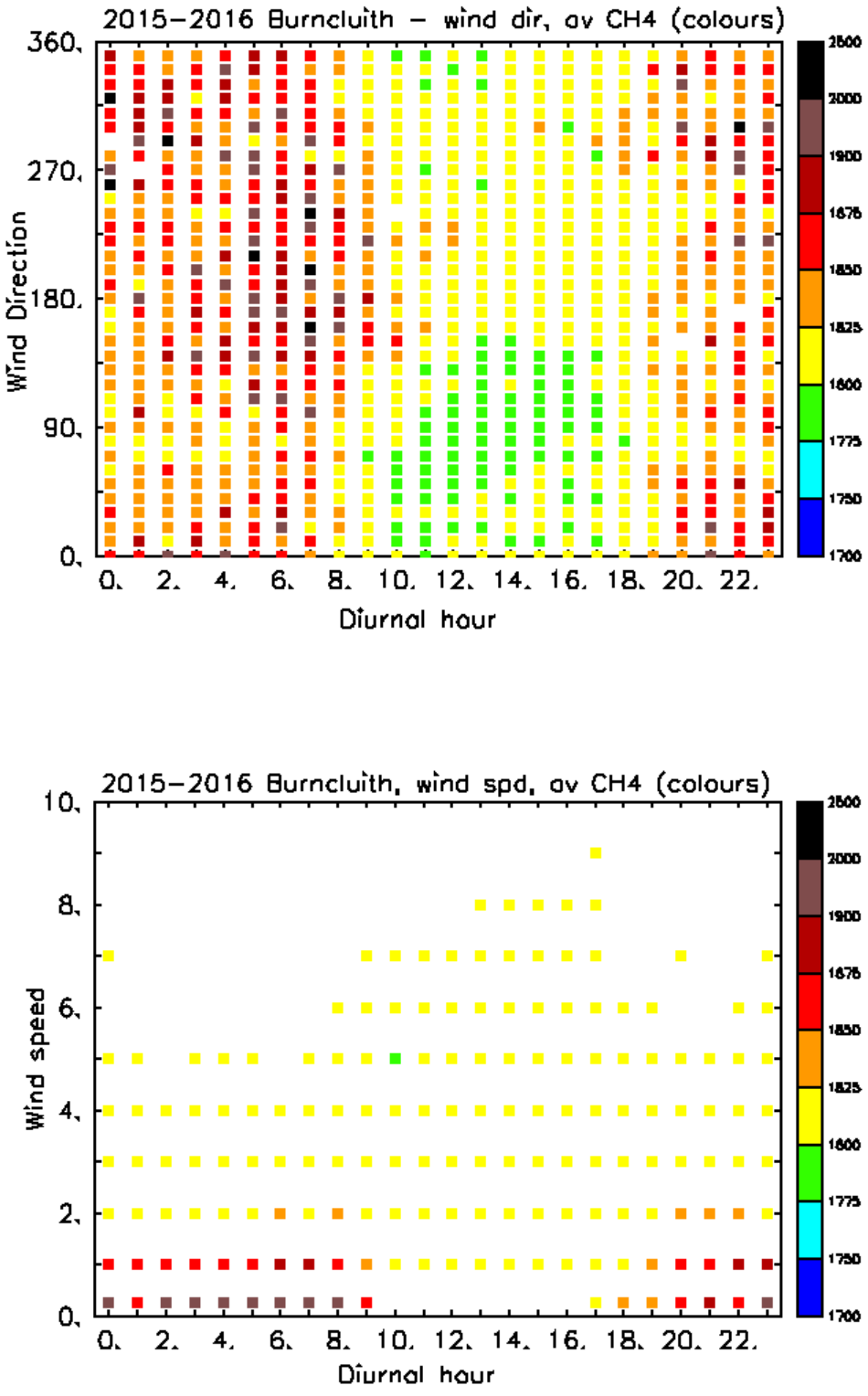

Figure 13. Variation of the average observed methane concentration (ppb) at Burncluith for 2015-2016 with diurnal hour and wind direction (degrees, top) and wind speed (ms^{-1}, bottom).

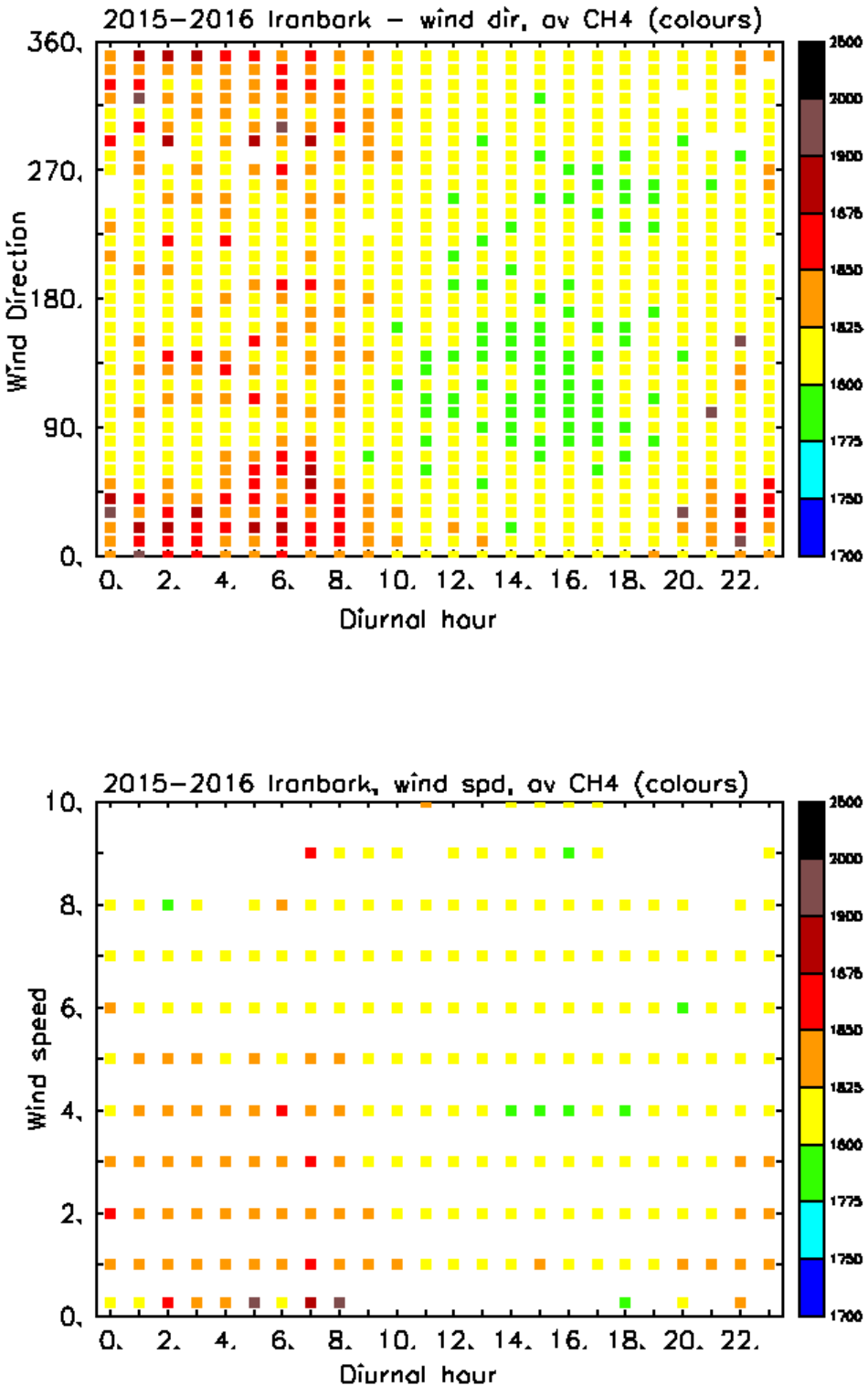

Figure 14. Variation of the average observed methane concentration (ppb) at Ironbark for 2015-2016 with diurnal hour and wind direction (degrees, top) and wind speed (ms^{-1}, bottom).

The winds at both Burncluith and Ironbark are predominantly north-easterly during October to January. From May to August the winds at Burncluith have a greater frequency of south-westerlies, while at Ironbark the frequency of south-westerlies is similar to that for north-

easterlies. Since Burncluith and Ironbark lie on a roughly north-east south-west line it seems reasonable to assume that under the right wind conditions enhanced concentrations of methane may be observed at Ironbark compared to those at Burncluith and less frequently the reverse. So when the winds at both sites are predominantly north-easterly enhanced methane concentrations might be observed at Ironbark and when the winds at both sites are predominantly south-westerly enhanced methane concentrations might be observed at Burncluith, if there are methane sources between the sites. Two months are chosen to investigate this: October 2015 for a north-easterly example and May 2016 for a south-westerly example.

Figure 15 shows selected methane concentration differences between Ironbark and Burncluith for October 2015 (top) and for May 2016 (bottom). For Figure 15 (top) only those hours were selected for which the wind at Burncluith was within 45 degrees of the wind at Ironbark and within 25 degrees of the vector line from Burncluith to Ironbark. This selection roughly correspond to the north-easterly winds at both sites. Hours for which the nighttime (2000-0800 h) wind speed at Burncluith was less than 1 ms^{-1} were also excluded. Figure 15 (bottom) follows the same selection criteria, except that the vector line is from Ironbark to Burncluith and nighttime hours for which wind speed at Ironbark was less than 1 ms^{-1} were excluded. This selection roughly corresponds to the south-westerly winds at both sites. Negative CH_4 concentration differences between Ironbark and Burncluith are seen in this case as Ironbark is upwind. More instances satisfy the criteria under north-easterly wind conditions in October than under southerlies in May. During October 2015 a number of time periods are shown of enhanced methane concentrations at Ironbark of up to 50 ppb and less frequently greater than 50 ppb. May 2016 shows a couple of periods of enhanced methane concentrations at Burncluith of up to 50 ppb and one occasion up to 100 ppb. This analysis suggests that when the winds are steady the methane concentration differences between Ironbark and Burncluith imply contributions from sources that are located between the two sites and that these differences could be used in modelling for the purposes of quantifying such sources. Concentrations simulated by forward modelling with TAPM using prescribed inventory sources (see Section 7) could be compared with observed concentrations, or sources in the region between the two monitoring stations could be estimated by inverse modelling (see below) using only a subset of the concentration data.

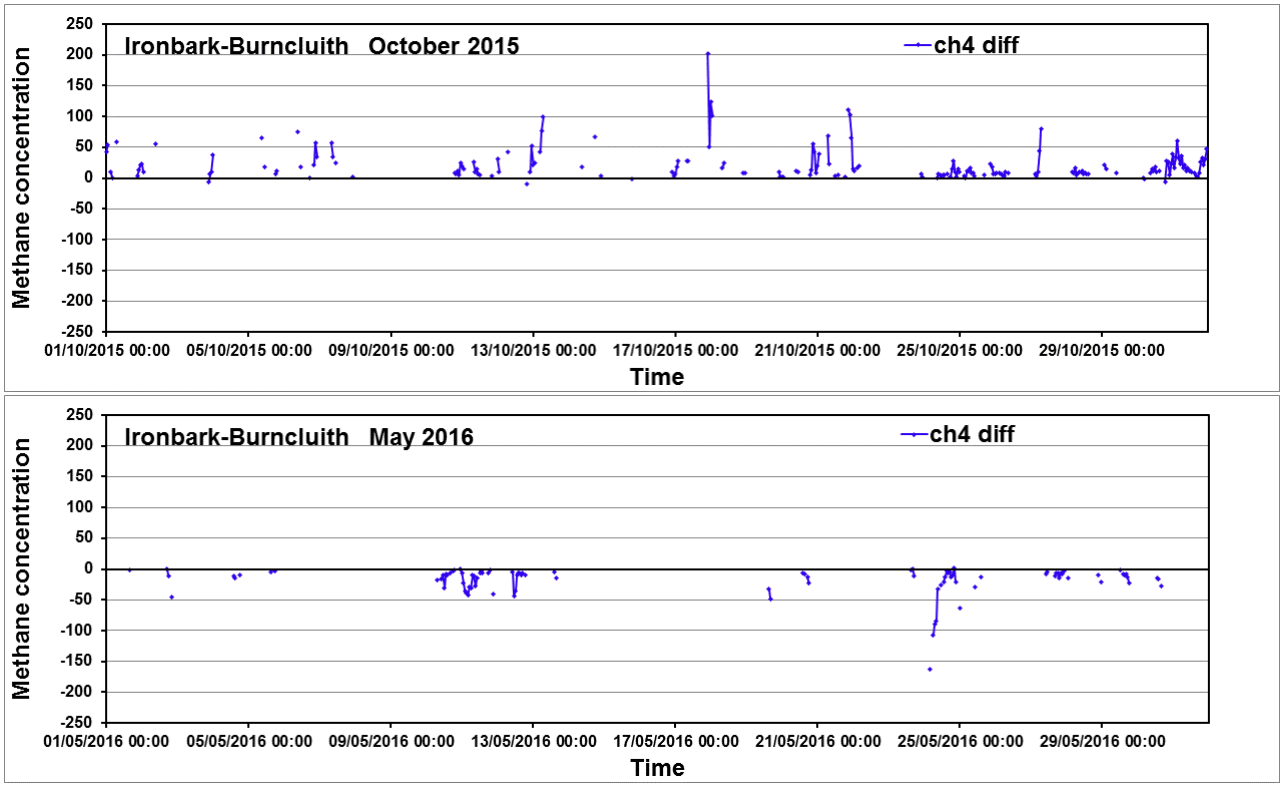

Figure 15. Methane concentration differences between Ironbark and Burncluith (positive when Ironbark concentration is greater) for when the wind direction was aligned with the two sites (allowing upwind-downwind differences to be calculated), for daytime hours, and night time if wind speeds were greater than 1 ms^{-1}. October 2015 (top) and May 2016 (bottom) were chosen for periods of pre-dominantly north-easterly winds and south-westerly winds respectively. See text for more details.

Selection of the data in this way provides background subtracted differences in methane concentrations from which the net methane emission across a large segment of the Surat Basin can be inferred. Further selecting periods of well mixed conditions avoids the difficulties in interpreting stable night time conditions. The selection process does however reduce the amount of data available for analysis, mitigated somewhat by the siting of the monitoring sites along dominant nodes of the wind roses. Because the focus of this monitoring is on trends in the net regional emission, rather than episodic point source emissions, the reduction in the data amount may not be too limiting.

5 Atmospheric dispersion modelling for source estimation

5.1 Modelling approaches

Atmospheric dispersion modelling calculates the dilution factor which provides a quantitative relationship between the emission from the source and its detection as concentration at a monitoring station. This relationship is often termed as the source-receptor relationship. Information about emission sources such as their release rates can, in principle, be inferred from measurements of their atmospheric concentrations coupled with the source-receptor relationship and available prior information about source characteristics.

There are two broad dispersion modelling approaches to determining emissions (Rao, 2007): forward modelling and backward modelling. In the first approach, concentration fields due to a source are predicted for a unit emission rate given the source location and meteorology of the area. For a single tracer source, a simple back calculation for the emission rate can be performed using the measured concentrations and the modelled dilution factor. However, if there are a large number of sources then the source-receptor relationship for each source needs to be pre-determined separately by using forward modelling and then used in an optimisation algorithm that minimises the difference between the measured concentrations and the modelled concentrations for a particular solution of source emission rates. The problem becomes even more difficult and computationally inefficient if, along with the source emission rates, the source locations are also not known, in which case every point in the spatial domain needs to be considered as a potential source and the corresponding source-receptor relationship determined, with the optimisation done over all these sources.

The second approach involves tracking plumes backwards in time from each monitor location. The value of modelled backward concentration at a particular point is equivalent to the relative contribution made by a potential source at that point to the measured concentration at the monitor. Thus a single backward source-receptor relationship field can be used to obtain the relative contributions made by each location point within the domain (whereas in the forward modelling each location point needs to be treated as a separate source and its plume transport determined). This is then combined with concentration measurements and an optimisation or inference method to yield source parameter information. If the number of potential sources to be considered is greater than the number of monitors, then the backward modelling is more efficient. Typically, in a source optimization scheme, e.g. that based on the Bayesian approach (described below), the number of source hypotheses that needs to be considered is larger than the number of available concentration measurement stations, and therefore the backward approach provides a significantly more efficient procedure. Another advantage of the backward approach is that it can be pre-run without regard to the details of the eventual source geometry. Forward modelling, on the other hand, is more deterministic and easier to formulate and comprehend.

Although the above dispersion modelling approaches are available for source quantification, the success of their application depends on a number of factors, such as the number and type of

source parameters to be estimated, the quantity and quality of concentration measurements available to constrain the sources, the capability of the dispersion model used for calculating the source-receptor relationship, the model, measurement and background concentration uncertainties, and the quantity and quality of prior information available on source characteristics.

We consider backward dispersion modelling for source estimation.

5.2 Backward dispersion modelling at regional scale

When formulating a backward dispersion model for local scale applications (< 10 km) where localised sources can be quantified, it is normally assumed that the meteorology over the averaging period of interest is steady and represents the whole domain if the terrain is relatively flat (e.g. Luhar et al., 2014). The backward model is typically driven by observed micrometeorological quantities (e.g. wind speed and direction, turbulence intensities and ambient stability) obtained from a single station in a study area.

When monitoring stations and the sources contributing to concentration signals at these stations are spatially far apart, the problem takes the dimension of regional scale (i.e. of the order of 100 km). Modelling emissions at regional scale is much more complex because surface conditions are usually inhomogeneous and the meteorology governing transport (and hence the source-receptor relationship) is spatially variable, and the source signals may not be strong enough to be detected. Unlike the local scale measurements which are focussed on a few localised sources, monitoring on regional scales represents integrated emissions from all source types contributing to measured methane concentration signals within the study area.

Modelling sources at the regional scale requires an appropriate plume transport model coupled with a meteorological modelling capability and an optimisation method (we refer to transport as being dispersion at regional scale). We have developed a backward transport modelling method that uses CSIRO's TAPM regional-scale model in backward time mode in order to provide the source-receptor relation required in the Bayesian inference inversion used for optimisation (described below).

5.2.1 Backward transport model description

We use The Air Pollution Model (TAPM v4.0) developed by CSIRO, which is an operational, inline, coupled prognostic meteorological and pollutant dispersion model (Hurley et al., 2005). TAPM has previously been applied to a variety of local- to regional-scale dispersion problems (e.g., Luhar et al., 2008; Zawar-Reza and Sturman, 2008; Luhar and Hurley, 2012). It is a forward model that estimates atmospheric concentrations due to given emission sources. It uses global input databases of terrain height, land use, leaf area index, sea-surface temperature, and synoptic meteorological analyses. We have developed a first version of a backward transport methodology based on TAPM which estimates emission rates of multiple sources given their locations and atmospheric concentrations. It requires further development, but the current setup is summarised as follows:

TAPM is first run for meteorology only (without dispersion) for the full period of interest (e.g. one year). The predicted horizontal wind components are reversed (i.e. sign change).

For dispersion, TAPM uses an Eulerian grid technique, with an optional Lagrangian particle-puff technique for the near field. TAPM dispersion is run backward in time for the full period of interest by using the previously modelled reversed wind components. The receptors are considered as sources for backward calculations and the resulting dispersion field is used as the source-receptor relationship, which is required for source estimation in the Bayesian inference method described below.

5.2.2 Bayesian inference for source estimation

The backward plume provides a means to map the source potentials of a geographical area, but it does not apportion the actual contribution of that source area to the concentrations measured at the receptors. An objective/optimisation methodology is required to do that. We use the Bayesian probabilistic or inference approach for that purpose. Given the source-receptor relationship from the backward transport model, model and observational uncertainties, and prior constraints on the source parameters, this approach updates our knowledge of source parameters as new concentration measurements become available and are taken into account. This overall methodology is referred as inverse modelling. In contrast to approaches that find a single optimal solution, the Bayesian approach explores all domains of plausible or permissible values of source parameters and assigns them probabilities. Thus it accounts for the fact that although many different source configurations may be plausible and consistent with the observed concentration measurements, some will be more probable than others. Applications of the Bayesian approach have been reported for a range of source estimation problems (e.g., Yee and Flesch, 2010; Humphries et al., 2012; Luhar et al., 2014) as well as network design studies (e.g. Ziehn et al., 2014). Depending on the type of concentration measurements and the amount of prior information available, the Bayesian approach can in principle be used to determine both the emission rates and locations of multiple sources, as well as other source characteristics.

Bayes' theorem or rule in the present context can be written as (Jaynes, 2003):

$$p(\mathbf{q}\,|\,\mathbf{c}) = \frac{p(\mathbf{c}\,|\,\mathbf{q})\,p(\mathbf{q})}{p(\mathbf{c})}, \qquad (1)$$

where $p(\mathbf{q})$ is the *prior*, which is the probability density function (PDF) of the source parameter vector **q** that encapsulates our knowledge of the source parameters before the receipt of the concentration measurements **c**; the *likelihood* function $p(\mathbf{c}\,|\,\mathbf{q})$ is the probability of observing the concentration data **c** for a particular **q** and is derived using a source-receptor relationship; $p(\mathbf{q}\,|\,\mathbf{c})$ is the *posterior*, which corresponds to the update of our prior knowledge of **q** through the modulation of $p(\mathbf{q})$ by the likelihood function which brings in the new information contained in the acquired concentration data **c**; and $p(\mathbf{c})$ is referred to as the *evidence* and is essentially a normalisation constant (Yee and Flesch, 2010). The likelihood function is derived using a source-receptor relationship obtained from a backward dispersion model, and its accuracy depends on how good the model is in explaining the concentration measurements. It mediates the transformation from the prior distribution to the posterior distribution through incorporating the information obtained in the acquired concentration data **c**. The Bayesian formulation takes into account measurement and model uncertainties, which are assumed to be normally distributed.

One advantage of the Bayesian approach is that any information known a priori about the source field can be taken into account through $p(\mathbf{q})$ to reduce the degree of underdeterminacy of the problem and help obtain a physically meaningful solution.

The prior PDF $p(\mathbf{q})$ needs to be specified. If the a priori information about the model parameters is Gaussian, then the posterior can be generally written in the matrix form as (Tarantola, 2005)

$$p(\mathbf{q}\,|\,\mathbf{c}) = \exp(-J)/Z_1 \tag{2}$$

where

$$J = \frac{1}{2}(\mathbf{c}_{\mathrm{m}}(\mathbf{q}) - \mathbf{c})^T \mathbf{C}_D^{-1}(\mathbf{c}_{\mathrm{m}}(\mathbf{q}) - \mathbf{c}) + \frac{1}{2}(\mathbf{q} - \mathbf{q}_{\mathrm{prior}})^T \mathbf{C}_M^{-1}(\mathbf{q} - \mathbf{q}_{\mathrm{prior}}), \tag{3}$$

$\mathbf{C}_D$ is the covariance matrix representing the addition of measurement and model uncertainties, $\mathbf{C}_M$ is the covariance matrix representing the uncertainty in the prior, the vector $\mathbf{q}_{\mathrm{prior}}$ is the prior source information, and Z_1 is a constant. The quantity J can be viewed as a cost function whose minimisation corresponds to the peak in the posterior, and hence to the solution.

The prior PDF can be assigned a uniform distribution when there is no prior information available about the source parameters. In that case the cost function is:

$$J = \frac{1}{2}(\mathbf{c}_{\mathrm{m}}(\mathbf{q}) - \mathbf{c})^T \mathbf{C}_D^{-1}(\mathbf{c}_{\mathrm{m}}(\mathbf{q}) - \mathbf{c}). \tag{4}$$

The posterior distribution $p(\mathbf{q}\,|\,\mathbf{c})$ provides probabilities of all the hypotheses about the values of the source parameters, and is integrated to obtain various mean source statistics of interest.

The TAPM source-receptor relationship obtained from the backward run is used as the likelihood function in the Bayesian probabilistic approach. To make the inverse modelling computationally faster, a Markov chain Monte Carlo (MCMC) method involving the Metropolis-Hastings algorithm is used to sample the posterior probability density function (PDF) of the source parameters (see Luhar et al., 2014). The methodology can determine emissions and their uncertainties from multiple sources whose locations, in the present configuration, are specified as prior knowledge.

5.3 Model setup for source inversion

The backward TAPM setup above was run for the Surat Basin area for the period 1 August 2015 to 31 August 2016. Two nested spatial domains were used (Figure 16): an inner domain of size 200 km × 200 with a horizontal grid resolution of 5 km × 5 km, and an outer domain of size 600 km × 600 with a horizontal grid resolution of 15 km × 15 km. The centre of the domains was -26°51' latitude, 150°29' longitude, with the corresponding Map Grid of Australia (MGA) coordinates being 249.930 E, 7027.697 N (Zone 56). The model domains partially fall within MGA Zone 55. All the distances reported here are relative to Zone 56.

Tracers were released from the Ironbark and Burncluith monitoring sites to generate the backward plumes with a nominal tracer emission rate of 100 g s^{-1}. A backward plume provides the

hourly source-receptor relationship required in the Bayesian analysis (which can then be scaled for any emission rate within the prior specification).

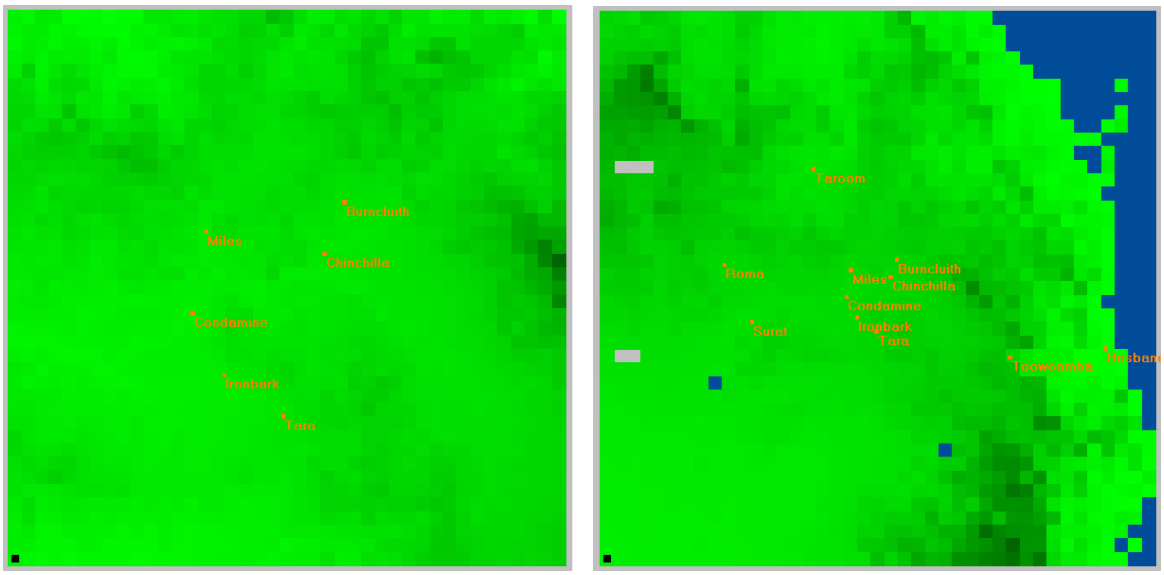

Figure 16. TAPM model domains used for meteorological and dispersion simulations. Left: inner-grid domain of size 200 km × 200 km with a horizontal grid resolution of 5 km × 5 km, right: outer-grid domain of size 600 km × 600 km with a horizontal grid resolution of 15 km × 15 km. Ironbark, Burncluith and other locations are shown. The colour shading represents topography (the darker the colour the higher the terrain elevation), and the blue colour is water.

5.4 Comparison of modelled winds with data

Inferring source locations and strengths using concentration data depends on the accurate simulation of the regional wind field by the atmospheric dispersion model. The TAPM winds can be tested at the two stations where we have meteorological measurements.

Figure 17 presents wind roses for Ironbark and Burncluith constructed using the TAPM generated winds from the model output at 10 m height for the inner nest (for the period August 2015 to July 2016). The model results at both sites are similar although TAPM predicts the frequency of winds from the east at Burncluith to be greater than those at Ironbark, and those from the east-northeast to be greater at Ironbark than Burncluith. There are also more frequent southerlies predicted at Ironbark.

Figure 18 shows wind roses for Ironbark and Burncluith based on the sonic anemometer measurements made at heights 5.8 m and 7.6 m, respectively. The two are qualitatively similar, with winds from the north-east quadrant being the most frequent. However, it is apparent that the winds from this quadrant are weaker at Burncluith than Ironbark.

Qualitatively the Burncluith modelled wind rose in Figure 17 is similar to that based on the observations in Figure 18, both show the prevailing winds from the north-east sector and smaller frequencies of wind from the other three sectors. The Ironbark modelled wind rose is also qualitatively similar to that based on the observations and both show similar winds to those at Burncluith.

There are also some significant differences between the observed and the predicted winds at both stations. At Burncluith the model underestimates the low wind speed events (< 2 m s^{-1}) from the north-east sector in particular and overestimates the higher wind speed events (> 4 m s^{-1}) from the northern sectors and the south-east sector. At Ironbark the model underestimates the higher wind speed events (> 4 m s^{-1}). The model predicts greater frequencies of easterly winds at both stations and underestimates the frequency of north-easterly winds at Ironbark.

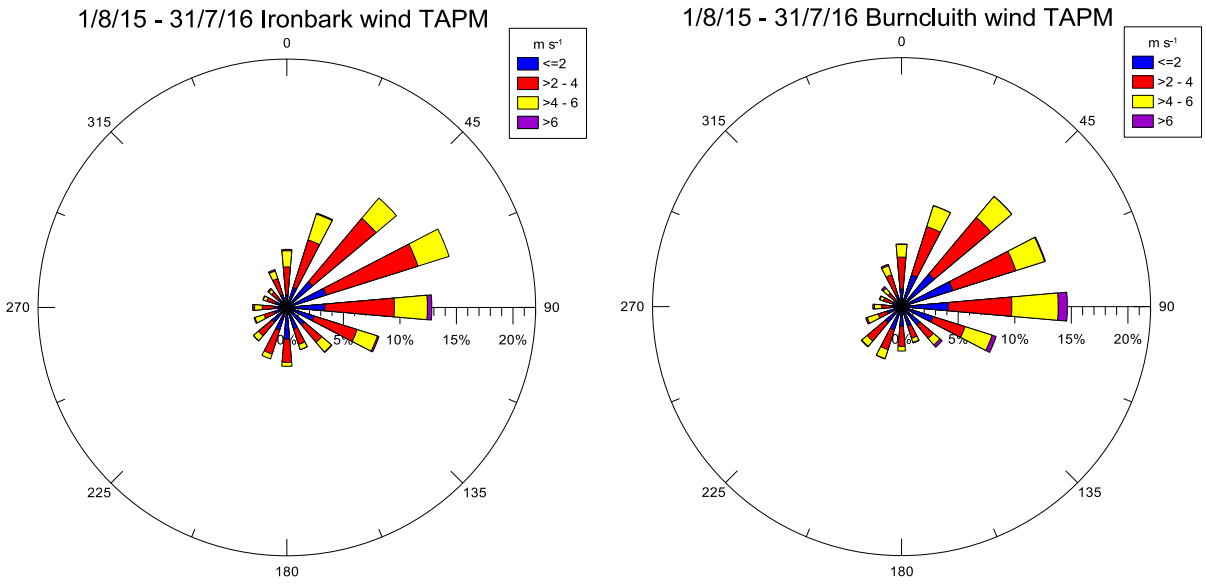

Figure 17. Modelled 10-m wind rose for the Ironbark and Burncluith monitoring sites (August 2015 to July 2016).

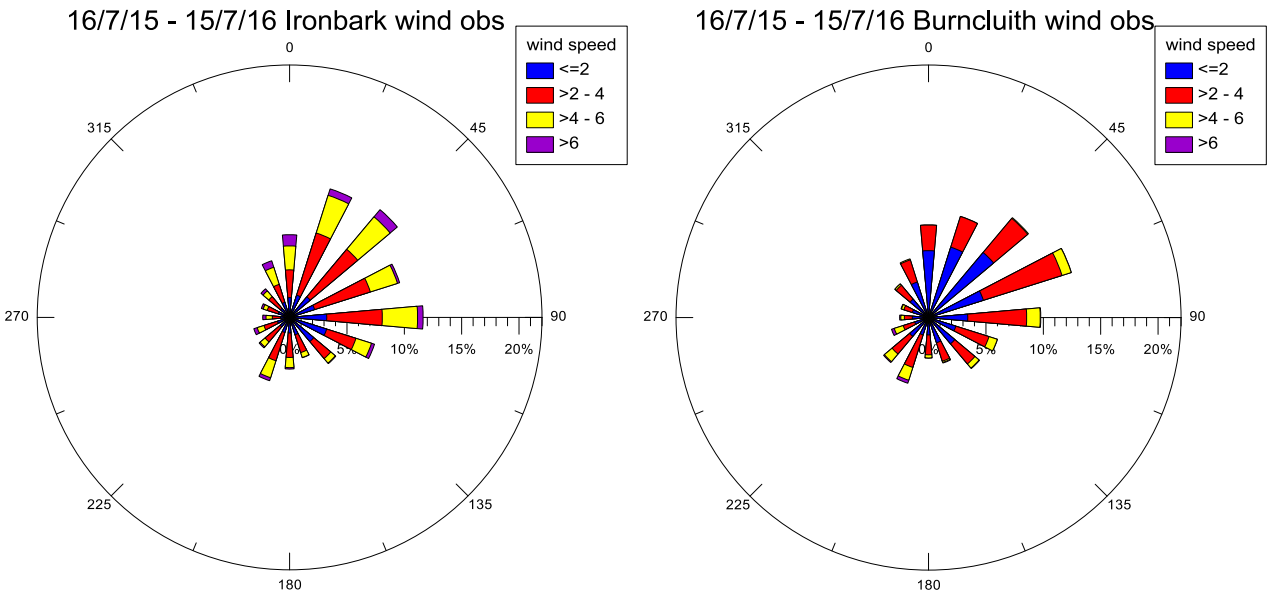

Figure 18. Measured wind rose for Ironbark and Burncluith (mid-July 2015 to mid-July 2016).

It is also useful to present the time series of winds. As an example, Figure 19 and Figure 20 show the observed and modelled hourly averaged wind speed and direction at Burncluith and Ironbark

for October 2015 and May 2016, respectively. The agreement between observed and modelled time series is qualitatively very good. During October 2015 (Figure 19) the winds are predominantly from the north-eastern sector at both sites and this is reproduced well in the model. The model overestimates the wind speed at Burncluith and underestimates the peaks in wind speeds at Ironbark. The agreement between the observed and modelled winds for May 2016 (Figure 20) is not as good as that for October 2015, mainly due to the observed winds being lighter and more variable at both sites than those during October 2015. Unlike October 2015 the observed winds in May 2016 are predominantly from the south-west as well as the north-east. The modelled wind speeds at Burncluith for May 2016 are closer to observations than those for October 2015.

TAPM has been quantitatively tested in numerous previous studies on meteorological and transport modelling from regional to local scale and has been found to perform on par with other similar models. Some of these comparisons have been reported in Hurley et al. (2005) and CSIRO (2004, 2005), and there are further comparisons within TAPM citation database (https://scholar.google.com.au/scholar?oi=bibs&hl=en&cites=13876071272134760358). We have not quantitatively evaluated TAPM for the Surat Basin in terms of statistical measures, but a qualitative comparison of the TAPM meteorological results presented above involving wind roses and time series for with previous model evaluation studies suggest that TAPM performance is comparable.

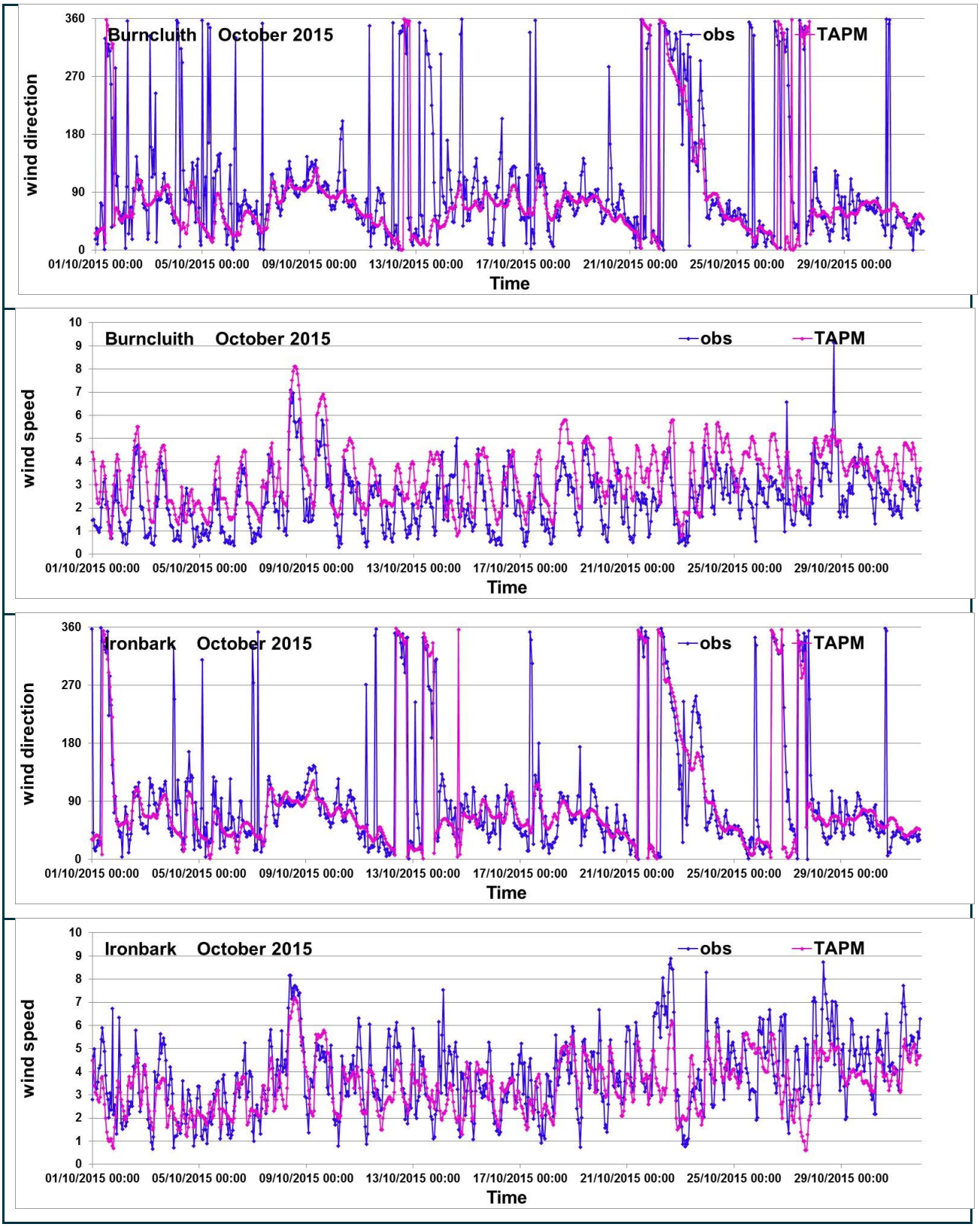

Figure 19. Hour mean wind speed and direction for October 2015 at Burncluith and Ironbark. Blue lines are the observations, and purple lines are the TAPM simulations.

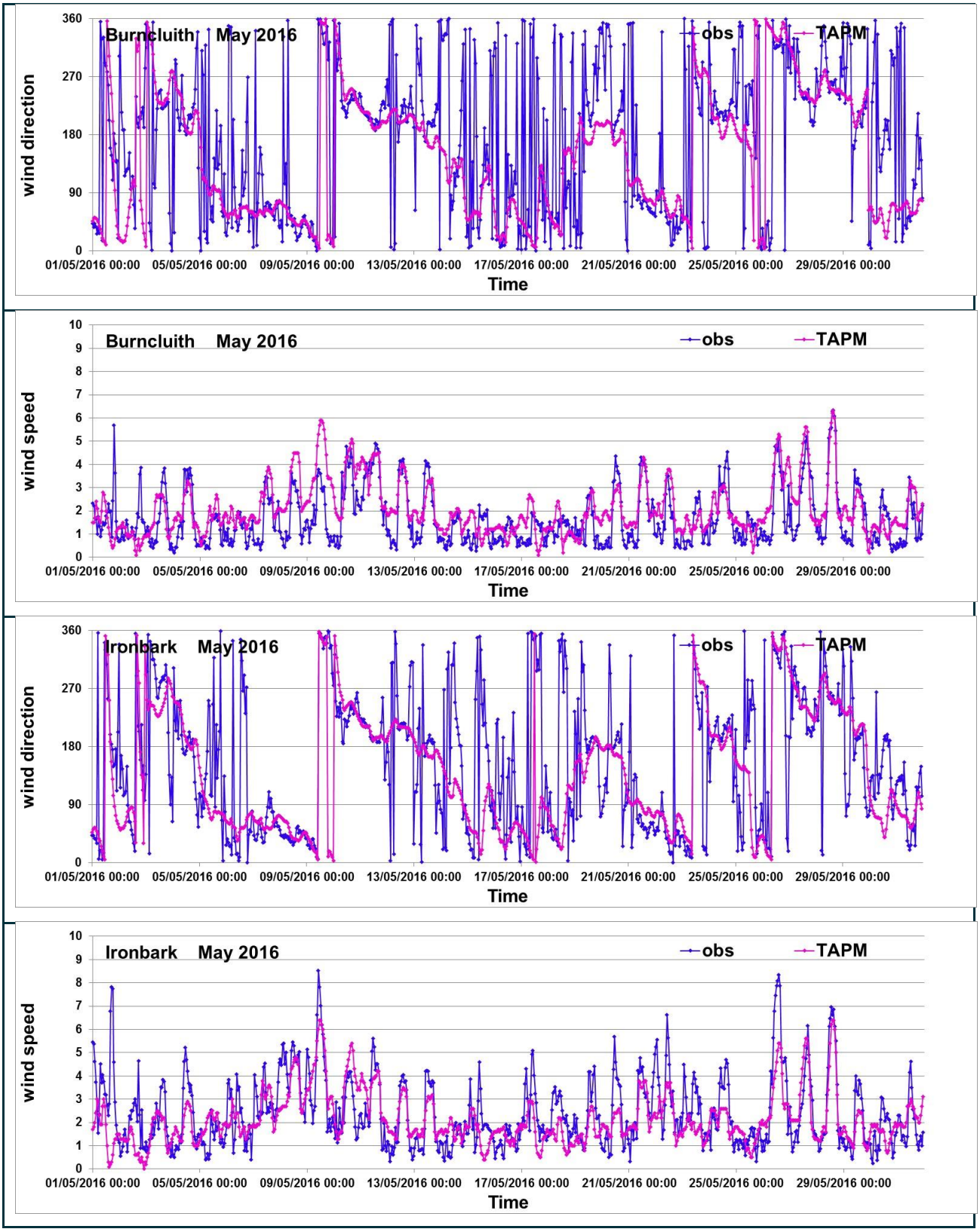

Figure 20. Hour mean wind speed and direction for May 2016 at Burncluith and Ironbark. Blue lines are the observations, and purple lines are the TAPM simulations.

5.5 Modelled backward plume footprints

The left plot in Figure 21 shows the modelled averaged backward tracer concentration field (μg m^{-3}) near the ground for Ironbark, and the right plot is that for Burncluith. Essentially such a plot for a monitoring station implies that the concentration value at any point within the domain is the (forward) concentration at the monitoring station if there were a source at that point emitting at 100 g s^{-1}. The backward concentration value at a particular point can also be interpreted, after a suitable normalisation, as the probability a source located at that point contributes to the concentration at the monitoring station. This demonstrates the considerable advantage of the backward approach over the forward approach, in that a large number of source hypotheses (which may include multiple sources with varying emission rates) can be explored using a single model run. The backward fields for the two sites are very similar, with large source contribution probabilities from the north-east quadrant followed by the south-east quadrant. This behaviour is consistent with the modelled wind roses at the two sites shown in Figure 17 in which the highest frequency of winds is from the north-east sector followed by the south-east sector. The backward concentration field for the Hopeland Air Quality station, which is located in between the Ironbark and Burncluith sites and may be used in future analysis, is also very similar (plot not shown).

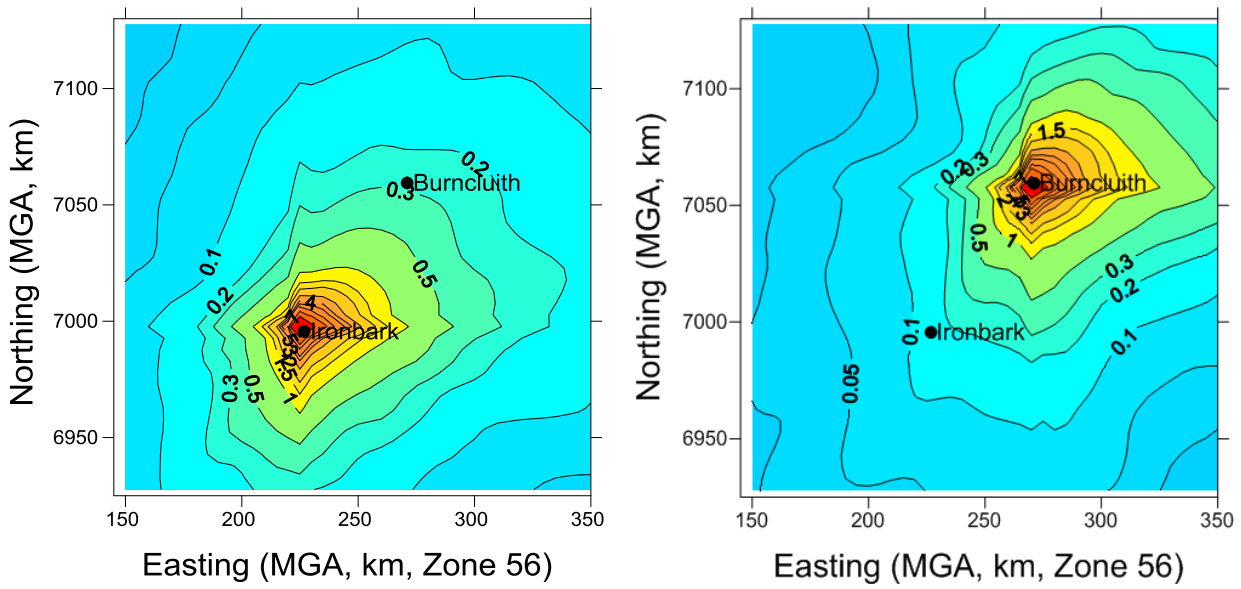

Figure 21. Left – Averaged modelled backward surface ground-level concentration field (μg m^{-3}) for the inner-grid domain, representing the source-receptor relationship, for the Ironbark site; Right – that for the Burncluith site. 1μg m^{-3} = 1.4 ppb.

5.6 Background concentration

The observed methane concentrations are total concentrations that include both background concentration and contributions from sources within the modelling domain. The background concentration needs to be subtracted from the observed concentrations to obtain methane signals that represent the contributing sources within the domain of interest. For the inverse analysis using all wind directions, background methane concentrations on a monthly basis were determined by averaging over the measured daily minimum concentrations and these were

subtracted from the methane data. Figure 22 presents the monthly variations of the calculated background concentration for the two sites, which are very similar, and are dominated by the seasonal variation. The seasonal variation in background atmospheric methane concentrations is driven mainly by varying destruction of methane by photochemical reactions in the atmosphere. The background monthly concentrations are chosen to try to best represent the regional background conditions which are a combination of the clean air concentrations at that latitude plus a contribution from regional sources outside the study area. For analyses of selected conditions when the wind is in line with the pair of monitoring stations (as discussed in Section 4.1), the upwind station measurement would provide a better background.

The standard deviation of the daily minimum concentrations averaged for all months is 5 ppb and is used as the uncertainty in the background concentration.

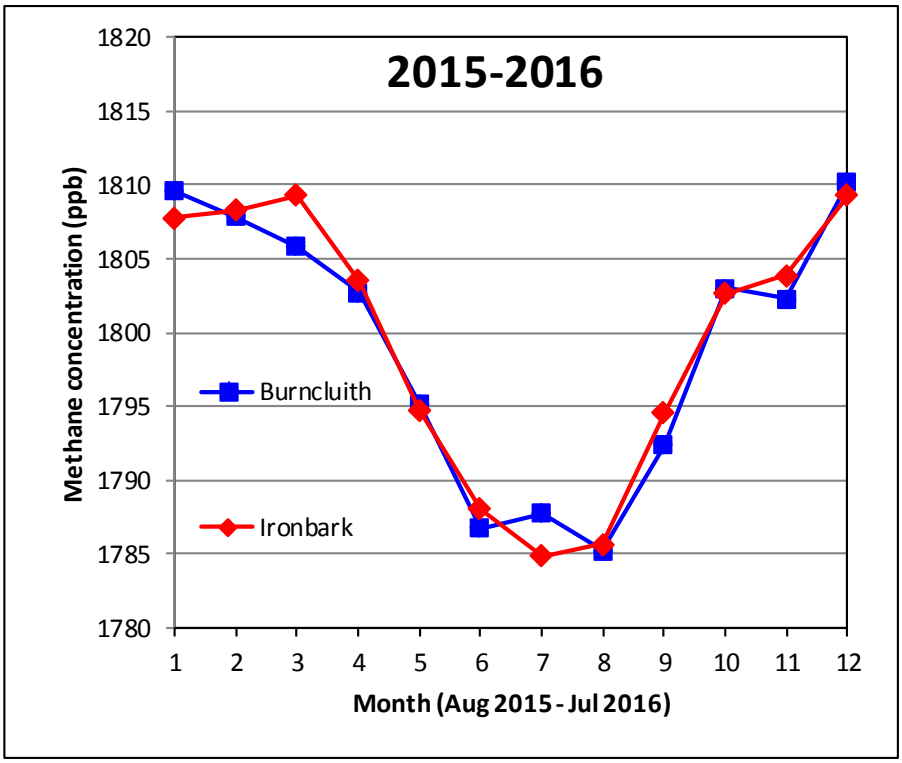

Figure 22. Monthly average of the measured daily minimum methane concentration (ppb) for Burncluith and Ironbark. These values are used as the monthly background concentrations in the modelling.

5.7 Emission determination

5.7.1 Model setup

The goal of the inverse Bayesian modelling is to infer methane source emissions across the domain given the observed methane concentrations and prior source knowledge. The methane concentration data include the influence of sources within the model domain. However, we do not exactly know the locations and types of all the sources within the modelling domain. One approach is to consider that the whole modelling domain is a potential source area and the task

then is to infer emission rates for various source areas within this domain using the measured hourly time series of methane concentration. For this purpose, we use the same inner-grid modelling domain of size 200 km × 200 with a resolution of 5 km × 5 km as used earlier, and consider a uniformly-spaced source array of 11 x 11 potential sources (so a total for 121 sources) within the model domains. In this model set up, the sources are treated as point sources and assumed to represent the gridded source areas. The simulation period was 1 August 2015 to 31 August 2016.

The background methane concentration was subtracted from the hourly-averaged measured concentrations. A background methane concentration uncertainty (σ_b) of 5 ppb and a prior of emission rate being less than 10,000 g s^{-1} for each of the 121 sources were specified. The ceiling on emission rate was chosen based on some trial and error such that the inferred emissions rates were well below this value. The ceiling could be increased further but doing that increases the uncertainty in the source estimation. Lowering the ceiling may put an artificial limit on potential sources whose emission rates could be higher than the ceiling value. A similar methodology has previously been applied when inferring emissions from open cut coal mining (Day et al., 2017).

The hourly source-receptor relationships obtained by the backward TAPM setup with Ironbark and Burncluith as the points of release were used as the likelihood function in the Bayesian analysis. Hence, the new information (over the specified prior) brought in by the likelihood function is the hour-mean concentration measurements for the selected period. All hourly methane concentrations available during the simulation period for which the 'signal' (i.e. the measured concentration minus the background value) was greater than σ_b were used. The modelling assumes that all sources emit at constant rate throughout the selected period, which enables the use of all valid hourly concentration data in one Bayesian calculation to determine the emission rates. The posterior PDF in the Bayesian analysis provides probabilities of all the hypotheses about the values of the source emission rate, and is integrated to obtain the mean and standard deviation of the emission rate.

High concentrations typically occur during low-wind (< 2 m s^{-1}) nocturnal inversion conditions, when the ambient stability is strong, turbulent mixing is suppressed, a greater degree of localised horizontal plume meandering occurs, and the flow field is most sensitive to the local terrain features. These are some of the most difficult conditions to simulate in a flow and dispersion model, particularly in a regional scale operational model such as TAPM. There are various reasons for that, including insufficient understanding of the physics of low-wind processes and their parameterisation in the model and limited horizontal and vertical resolutions (e.g. Luhar and Hurley, 2012, and references therein). High concentrations of methane at night are evident in the data from Burncluith, and to a lesser extent from Ironbark, which were presented earlier (Figure 13 and Figure 14). It was also clear that the frequency of nocturnal low winds predicted by TAPM was smaller than that observed at Burncluith. One option to circumvent the issue is to consider only daytime hours as discussed earlier. We consider the period 0900–1900 (end hours).

The inverse modelling methodology has been extended to include concentration data from more than one location. We consider three separate inverse modelling cases involving: 1) only Ironbark data, 2) only Burncluith data, and 3) both Ironbark and Burncluith data. The initial source inference results are presented below.

5.7.2 Initial results

Figure 23 shows the distribution of the total mean methane source emission rates (g s^{-1}) inferred by the model based on the methane measurements at Ironbark. Note that all types of methane source are represented in the model-inferred emission estimates. The model suggests some source regions near Ironbark that have relatively high emission rates, particularly those to the north, east and south-west of the station. There are some prominent inferred source regions close to the boundary of the domain.

Figure 24 is the model inferred source distribution when the methane measurements from Burncluith are used. There are some source regions inferred in the vicinity of Burncluith which were not as prominent in Figure 23. There are some changes to the source distribution north of Ironbark, and some of the inferred sources near the domain boundary are less intense than in Figure 23. Given the considerable distance between the two sites, it is likely that Burncluith would sample methane contributions from some sources better than would Ironbark and vice versa depending on how the real sources are spatially distributed and how the emissions are transported by the meteorology. This could then impact the source inference from the model, and this is apparent in Figure 23 and Figure 24. However, generally speaking, there is a qualitative similarity between the two modelled source distributions in terms of the order of magnitude of emissions and their locations.

In general, the greater the quality and quantity of information going into the Bayesian analysis the better the quality of source inference. Figure 25 is the inferred source distribution when the methane concentration measurements from both Ironbark and Burncluith are used jointly in a single Bayesian run. By considering two spatially separate stations with concentration data of the same quality increases the sample size and improves source triangulation, thus strengthening the quality of source determination. Figure 25 shows some characteristics that are similar to Figure 24 (i.e. source areas around Burncluith) and a 'readjustment' of sources around Ironbark compared to the previous two plots.

If some actual sources are located outside the modelling domain that contribute significantly to the measured methane signal above the selected background value, then the present simulation would not handle that situation properly. One option would be to consider a bigger domain.

We plan to compare the inferred source distribution with independent information on sources in the area and examine the model uncertainties. As an example, the estimated emission rate for the dominant Condamine River seeps located almost midway between Chinchilla and the Hopeland Air Quality (AQ) station is 12–24 gs^{-1} (Day et al., 2015; B. Sherman personal communication), whereas the inferred emission rate for the corresponding grid cell in Figure 25 is much lower, at around 1 gs^{-1}. There are various factors that could impact the inferred locations of the methane sources compared to the inventory sources. For example, any shift in the modelled wind direction compared to the observed can cause a shift in the estimated source location. There are significant differences between the modelled and observed wind directions (see Figure 17 and Figure 18), and, therefore, it is possible that the inferred source locations could have deviated somewhat. In Figure 25, the grid cells immediate to west and south of the grid cell within which the Condamine River seeps lie show inferred emission rates of approximately 100 gs^{-1}. It is possible that Condamine River seeps are accounted for by the model in one of those cells due to the wind direction differences. It would be useful to conduct a sensitivity study in which the dispersion

model is run in forward mode with the seeps as the source to gauge whether the predicted levels of methane at the two monitors are indeed detectable. Similarly, another forward modelling simulation could be carried out in which all the inferred emissions are used to compute methane concentrations at the two monitors to check whether the modelled concentrations agree with the observations.

When studying particular sources such as Condamine River seeps, a smaller model domain with higher resolution coupled with the methane signals, if available, from an upwind-downwind concentration difference from two monitors (described below) and better priors could provide better source estimates than the larger scale, regional modelling conducted above.

The calculation of background concentration is important especially for sources distant from the monitor locations because the concentration contributions from such sources could be small and within the uncertainty of the background concentration, such that these sources would be hard to quantify. Thus the sensitivity of source inference to the background concentration will need some additional work.

The above inverse calculations are a first attempt at the estimation of region-wide methane emissions in the Surat Basin. The modelling results presented here provide a useful demonstration of the capability and potential of the Bayesian inference coupled with the calculation of the source-receptor relationship using the backward dispersion approach for source estimation at regional scale.

There are various assumptions and parameter uncertainties in the modelling, which include the assumption that all sources emit at constant rate throughout the selected period. Modelled meteorology is an approximation of the real-world meteorology, and differences between the two would cause differences in plume transport, contributing to prediction accuracy. We have considered 121 point source locations for source inference. Other source configurations (e.g. area source) could also be considered with further model development. We could also look at adding other sites (e.g. Hopeland Air Quality Station) depending on the suitability and consistency of the methane data from there, and perform sensitivity analyses involving background concentration criterion, daytime hour selection, grid resolution and domain size.

Inverse modelling could also be undertaken to better quantify the sources in between Ironbark and Burncluith under steady wind conditions for which one of the two stations can be considered as the background (or upwind) station and other as the downwind station measuring the upwind source contributions, as shown for example in Figure 15. This setup has the advantage of having a well-defined background that allows more accurate determination of the signal from emissions in the region between the stations. Such an upwind-downwind strategy was followed by Luhar et al. (2014) at the local scale.

Once the accuracy of the inverse modelling approach has been sufficiently verified it could be used to compare with emissions inventories. Forward regional modelling would use bottom-up emissions from the methane emission inventory supplied by Katestone Scientific (see below), which would help quantity the CSG component of emissions in conjunction with the inverse modelling.

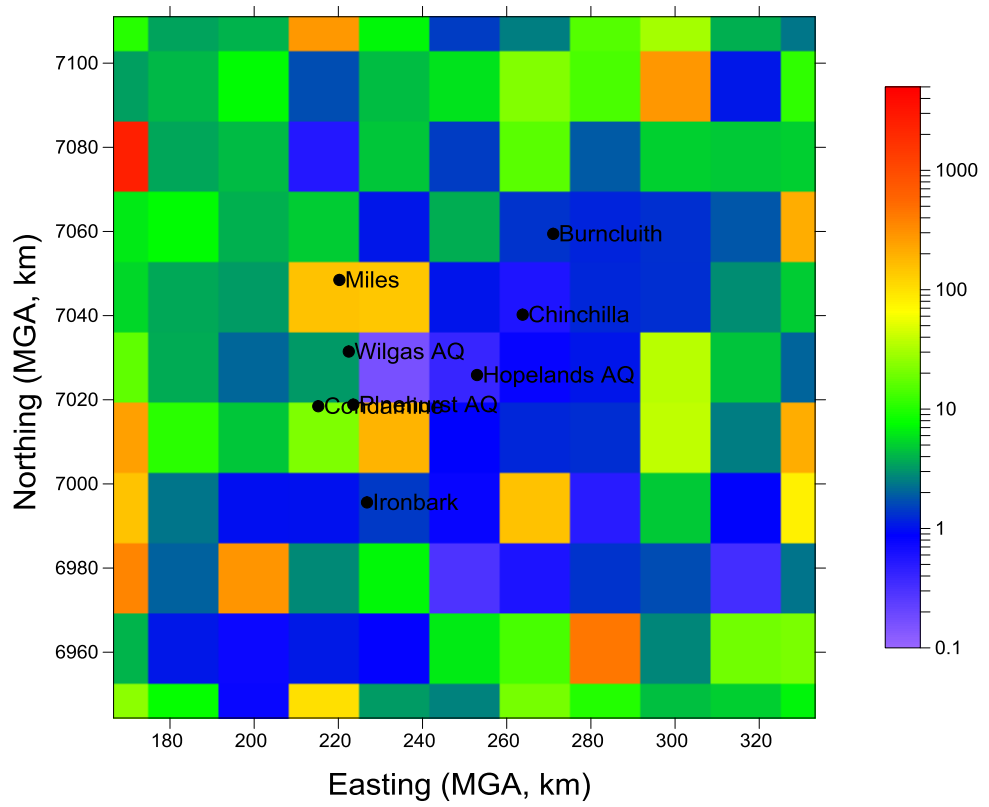

Figure 23. Methane emission rates (g s^{-1}) inferred by the inverse model for a uniformly-spaced source array of 11 x 11 sources (a total of 121 source areas) using the measured hourly-averaged methane concentration for 0900–1900 h (end hours) at Ironbark for August 2015 – August 2016. Note the logarithmic emission scale. The site locations are also shown.

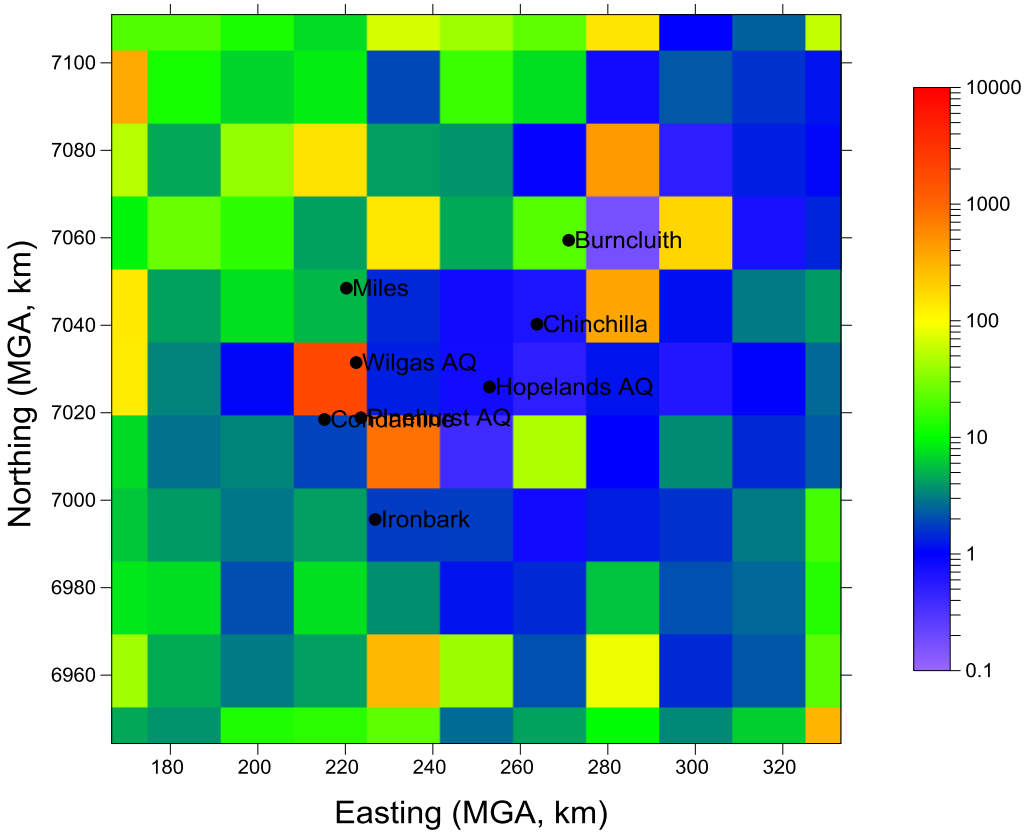

Figure 24. Methane emission rates (g s^{-1}) inferred by the inverse model for a uniformly-spaced source array of 11 x 11 sources (a total of 121 source areas) using the measured hourly-averaged methane concentration for 0900–1900 h (end hours) at Burncluith for August 2015 – August 2016. Note the logarithmic emission scale. The site locations are also shown.

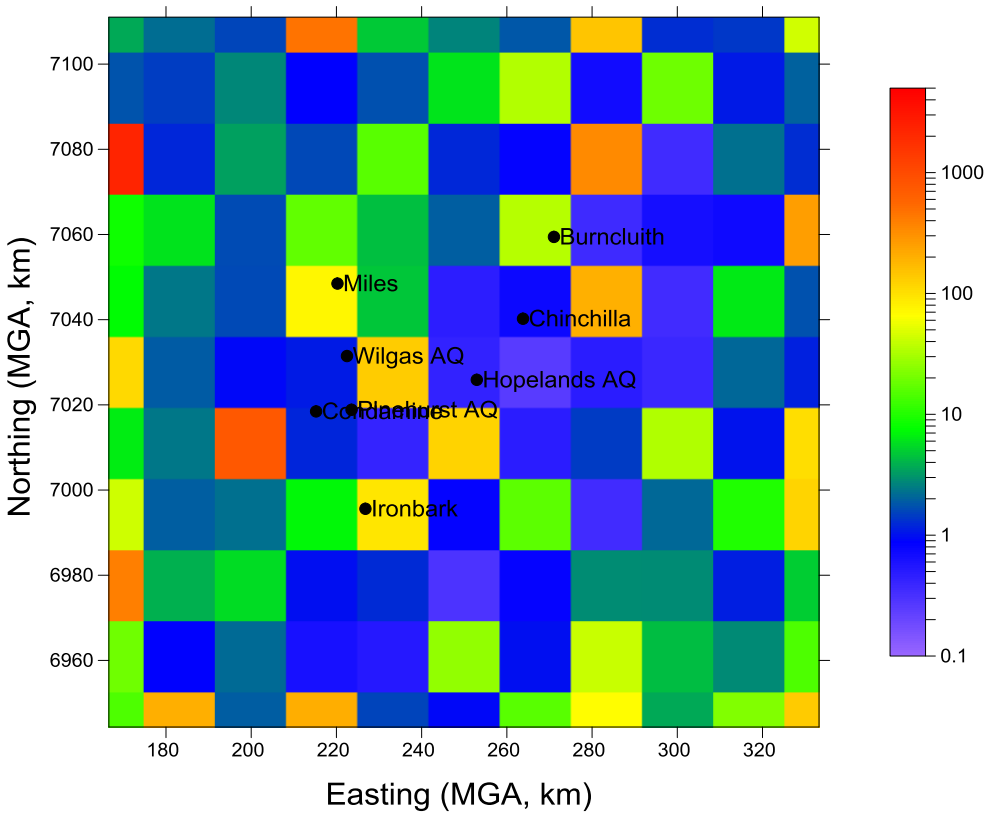

Figure 25. Methane emission rates (g s^{-1}) inferred by the inverse model for a uniformly-spaced source array of 11 x 11 sources (a total of 121 source areas) using the measured hourly-averaged methane concentration for 0900–1900 h (end hours) at both Ironbark Burncluith for August 2015 – August 2016. Note the logarithmic emission scale. The locations various sites are also shown.

6 Mobile ground surveys

Mobile ground surveys have been conducted over a wide region from between Chinchilla and Roma to locate abandoned boreholes and other potential methane land seeps. Approximately 1000 abandoned boreholes sites have been surveyed where downwind methane concentrations have been measured and local wind speed and direction data used to determine whether or not methane is leaking from the boreholes. Most of the boreholes examined are old coal exploration holes, but there have also be numerous plugged and abandoned CSG wells included in the dataset. So far the majority of sites examined have shown no methane emissions. However, a handful of sites have shown some level of emission. At these sites, methane emission rates have been estimated using surface flux chambers (used during Phase 2 of the GISERA Methane Project) or a tracer gas method.

In addition to the boreholes, a number of small terrestrial seeps have been identified. These sites do not correspond to known locations of abandoned boreholes (although this possibility has not yet been ruled out) and often show signs of vegetation changes compared to adjacent areas where there is no methane seepage. Emission rate estimates have been attempted at several of these sites – work on quantifying these emissions is ongoing.

Data from these surveys will be used to improve the regional methane inventory that is currently under development, see below.

7 Preparation of methane emissions inventory

An inventory of methane sources is being developed with input from consultants Katestone. This will be used to help quantify the contribution of methane emissions from the existing methane sources so that CSG sources may be better identified and their emissions estimated from the inverse modelling of the continuous ground based concentration measurements.

Source categories in the inventory so far include motor vehicles (exhausts), power stations (stack emissions, gas fired and coal fired), agriculture (feedlots, piggeries, poultry, grazing cattle, water wells), coal mining (fugitives from open cut mines, exploration wells, material handling, combustion), sewer treatment, landfills, and geological land and river seeps. They are derived from state, national and international databases, from the GISERA mobile methane monitoring tasks, and from industry. Emissions from other sources will be included in the future, in particular, coal seam gas activities, which are being compiled from industry and Queensland Government sources.

The domain is 345 km east-west and 344 km north-south, centred near Miles. The grid cells are 1 km by 1 km. Time variations on diurnal and seasonal timescales are included for some sources.

Figure 26 shows the preliminary methane emissions across the inventory domain for non-CSG sources only. The inset corresponds to the inner domain for the inverse modelling reported above.

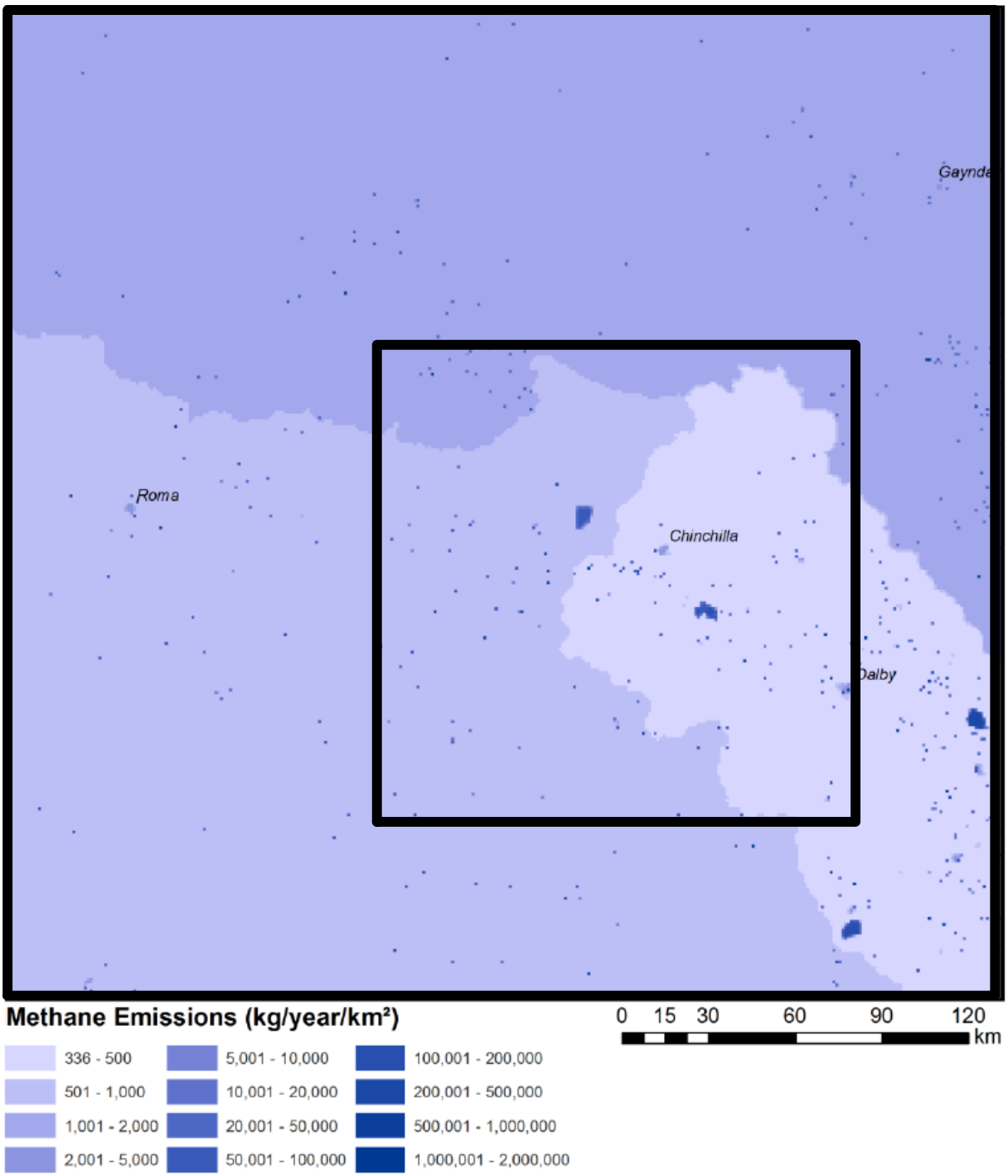

Figure 26. Map of methane emissions, preliminary inventory data for non-CSG sources only. The inner domain for the inverse modelling is inset.

8 Discussion, conclusions and further work

The results presented in this interim report demonstrate the potential to infer regional emissions of methane across the Surat Basin with an inverse modelling approach, using a combination of methane concentration measurements and plume transport modelling. To our knowledge, this study is the first to infer regional emissions of methane in this way.

The Ironbark and Burncluith monitoring stations provide the long term and continuous methane concentration measurements required for the inversions. Absolute calibration of the measurements allows concentration differences between the sites, coupled with appropriately calculated background concentrations, to be calculated with sufficient precision that emissions can be inferred. The stations are suitably located to record concentration signals from across the region without being dominated by the effects of nearby sources. Filtering of spikes in methane concentrations effectively removes unwanted signals from grazing cattle occasionally passing upwind of the monitors. The effect on hour mean concentrations (maximum corrections of about 10 ppb at Ironbark and 50 ppb at Burncluith) can be significant compared to the signals caused by methane emissions in the region of interest. Further selection of daytime-only measurements for inferring emissions avoids complications of modelling during strong nocturnal atmospheric stability.

The inversion gives stable and consistent solutions from run to run, giving confidence in the computational techniques. We used Bayesian inference coupled with the calculation of the source-receptor relationship using the backward dispersion approach to infer the source information. This requires accurate simulation of the wind field. The region is conducive to atmospheric modelling, being relatively flat, and the TAPM winds generally compare well with the observed winds. However, the differences at each of the two monitoring stations and likely elsewhere in the model domain could lead to errors in the inversion results. The modelled-observed differences in winds and their effect on the inversion warrants further investigation.

Several tests and potential improvements could be made to the inverse modelling. It could be validated by using the source emissions and locations inferred by the model to simulate concentration time series at each monitoring station by running TAPM in forward mode. These can then be used as “synthetic data” in a further inversion to see how well the input source information is recovered.

The methane emissions inferred from the inversion are also sensitive to the choice of background concentration, which, for the general inversion of sources across the domain was found from the monthly average of the measured daily minimum methane concentration measured at the two sites. The meteorological measurements at Ironbark and Burncluith confirm the relatively high frequency of north east and south west wind directions which were identified in the modelling and led to the station placements. Methane concentration differences between the two stations during selected conditions when winds are along this axis give the true background-subtracted concentration enhancement for that sector, which should allow emissions between Ironbark and Burncluith to be accurately modelled. We plan to explore this in the next stage of the project.

With the inverse modelling improved as described above and validated using synthetic emissions and using individual source emissions that are independently quantified, the inferred ("top-down") emissions can then be compared with the inventory ("bottom-up") emissions. It is important to note that each approach is an estimation and has uncertainties. The inverse modelling is limited by having only two monitoring stations across a wide area that contains many methane sources. It makes assumptions about the sources that contribute to the measured concentrations, including that they are steady in time and are all contained within the model domain. It relies on the source-receptor relationship (derived from the transport model) being accurate across the region. These are typical difficulties of inverse modelling. Ways to reduce some of the uncertainties are described above (for example, selecting optimum meteorological conditions, focussing on the sector in between the two monitors). Inventory emission estimates can be uncertain due to errors and assumptions in emission factors, activity data and scaling-up. The inventory used here will include measured emissions for some sources such as coal mines, river seeps and land seeps as they become available. Further, not all source types are included in the emissions inventory (such as biomass burning, which is sporadic, and ground water wells, for which no emission factors are available). The inverse modelling, on the other hand, will likely infer emissions from all source types combined but is not able to discriminate between them, unless they are geographically discrete at the resolution of the inversion grid and sufficient information about them is contained in the measurements. Together, the top-down and bottom-up methods are complimentary and can provide regional emissions with reduced uncertainties.

References

Bai, M., Griffith, D.W.T., Phillips, F.A., Naylor, T., Muir, S.K., McGinn, S.M., Chen, D. Correlations of methane and carbon dioxide concentrations from feedlot cattle as a predictor of methane emissions. Animal Production Science 56, 108-115, 2014.

Day, S., Dell 'Amico, M., Etheridge, D., Ong, C., Rodger, A., Sherman, B. et al. Characterisation of regional fluxes of methane in the Surat Basin, Queensland. Phase 1: A review and analysis of literature on methane detection and flux determination. Canberra: CSIRO; 2013.

Day, S., Ong, C., Rodger, A., Etheridge, D., Fry, R., Dell'Amico, M., Sestak, S., Williams, D., Loh, Z., and Barrett, D. Characterisation of regional fluxes of methane in the Surat Basin, Queensland: Phase 2: A pilot study to detect and quantify methane sources. Canberra: CSIRO; 2015.

Day, S., Luhar, A., Etheridge, D., Hibberd, M., Thatcher, M., Loh, Z., Noonan, J., Marvig, P., Weir, S., Halliburton, B., Improving Methods for Quantifying Fugitive Emissions from Open-Cut Coal Mining, CSIRO, Project Number: C24017, 2017.

DNRM (2014). Queensland's coal seam gas overview, January 2014, prepared by Queensland Department of natural Resources and Mines. http://mines.industry.qld.gov.au/assets/qld-miningupdate/csg.pdf, accessed 18 Dec 2014.

Etheridge, D. M., S. Day, M. F. Hibberd, A. Luhar, D. A. Spencer, Z. M. Loh, S. Zegelin, P. B. Krummel, E. van Gorsel, D. P. Thornton, R. L. Gregory, C. Ong and D. Barrett. Characterisation of Regional Fluxes of Methane in the Surat Basin, Queensland - Milestone 3.1 GISERA Greenhouse Gas Research – Phase 3. CSIRO, Australia, 2016.

Humphries, R., C. Jenkins, R. Leuning, S. Zegelin, D. Griffith, C. Caldow, H. Berko, and A. Feitz. Atmospheric tomography: A Bayesian inversion technique for determining the rate and location of fugitive emissions, Environmental Science and Technology, 46, 1739–1746, 2012.

Hurley P. J., Physick, W. L., Luhar A. K. 'TAPM: a practical approach to prognostic meteorological and air pollution modelling', Environmental Modelling and Software 20:737–752, 2005.

Jaynes, E. T. Probability Theory: The Logic of Science, Cambridge University Press, Cambridge, UK, 753 pp., 2003.

Lawson, S.J., Hibberd, M and Keywood, D. GISERA Ambient Air Quality in the Surat Basin – Overview of study design. CSIRO, Australia. 2017.

Loh, Z. M., R. M. Law, T. Ziehn, M. V. van der Schoot, P. B. Krummel, L. P. Steele, D. M. Etheridge, D. A. Spencer, R. L. Gregory, R. L. Langenfelds and A. R. Stavert, in Atmospheric Composition & Chemistry Observations & Modelling Conference incorporating the Cape Grim Annual Science Meeting 2016 [abstract], 16-18 November 2016, Stanley, Tasmania, N. Derek and P. B. Krummel (eds.), Bureau of Meteorology and CSIRO Oceans and Atmosphere, Climate Science Centre, Melbourne, Australia, page 28, 2016.

Luhar A. K., Etheridge D. M., Leuning R., Loh Z. M., Jenkins C. R., Yee E.. Locating and quantifying greenhouse gas emissions at a geological CO_2 storage site using atmospheric modeling and measurements, Journal of Geophysical Research: Atmospheres 119:10959–10979, 2014.

Luhar, A. K., Mitchell, R. M., Meyer, C. P., Qin, Y., Campbell, S., Gras, J. L., Parry, D. Biomass burning emissions over northern Australia constrained by aerosol measurements: II–Model validation, and impacts on air quality and radiative forcing. Atmospheric Environment 42, 1647–1664, 2008.

Luhar, A. K., Hurley, P. J. Application of a coupled prognostic model to turbulence and dispersion in light-wind stable conditions, with an analytical correction to vertically resolve concentrations near the surface. Atmospheric Environment 51, 56–66, 2012.

Rao, K. S. Source estimation methods for atmospheric dispersion. Atmospheric Environment 41, 6964–6973, 2007.

Tarantola, A. Inverse Problem Theory and Methods for Model Parameter Estimation. Society for Industrial and Applied Mathematics, Philadelphia, 342 p., 2005.

Yee, E., and T. K. Flesch. Inference of emission rates from multiple sources using Bayesian probability theory, Journal of Environmental Monitoring, 12, 622–634, 2010.

Zawar-Reza, P., Sturman, A. Application of airshed modelling to the implementation of the New Zealand National Environmental Standards for air quality. Atmospheric Environment 42, 8785–8794, 2008.

Ziehn, T., Nickless, A., Rayner, P. J., Law, R. M., Roff, G., Fraser, P.. Greenhouse gas network design using backward Lagrangian particle dispersion modelling – Part 1: Methodology and Australian test case. Atmospheric Chemistry and Physics 14, 9363–9378, 2014.

Appendix.

CONTACT US

t 1300 363 400
+61 3 9545 2176
e enquiries@csiro.au
w www.csiro.au

FOR FURTHER INFORMATION

David Etheridge
t +61 3 9239 4590
e david.etheridge@csiro.au

Stuart Day
t +61 2 4960 6052
e stuart.day@csiro.au